Chair of Hydrological Modeling and Water Resources

Albert-Ludwigs-University of Freiburg

Marvin Lorff

Deciphering the impact of climate and hydrology on recession-based discharge analysis

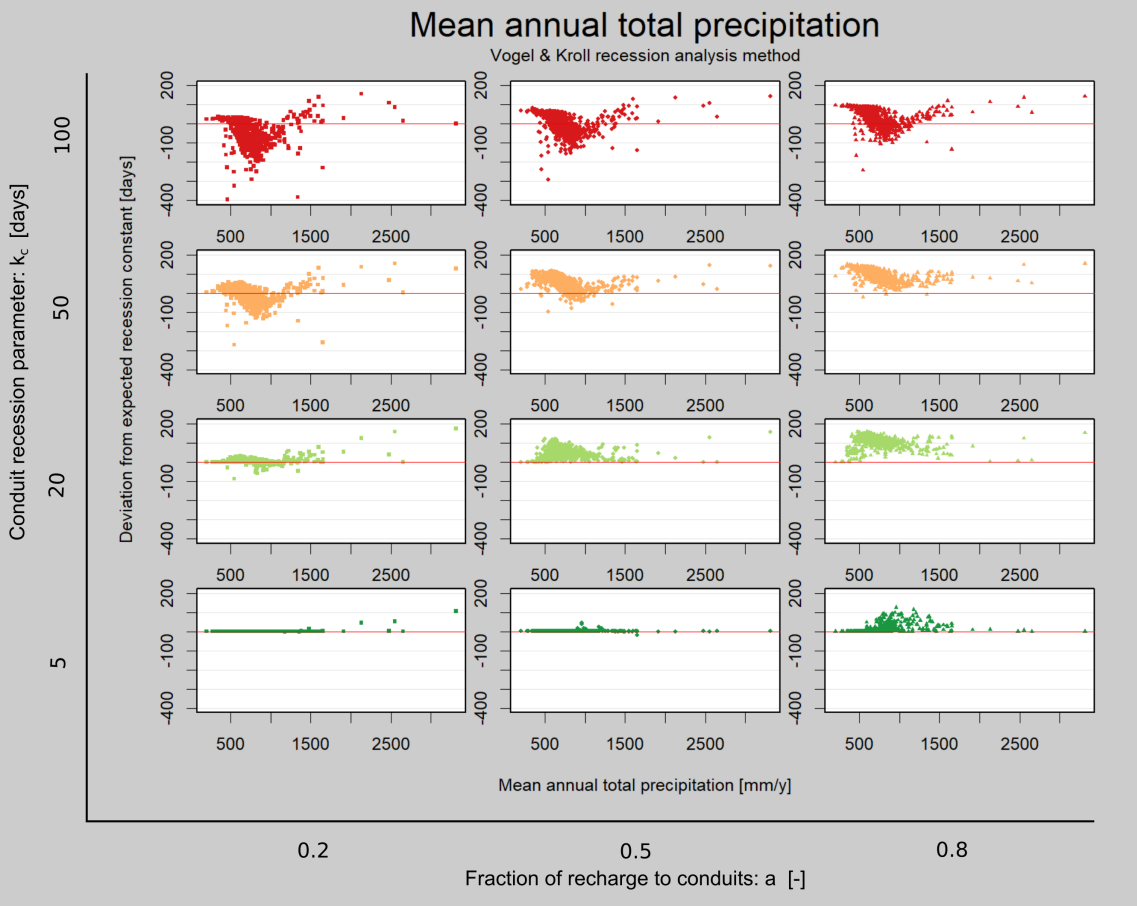

MSc-Thesis under the guidance of JProf. Dr. Andreas Hartmann

Freiburg i. Br., Mai 2020

Chair of Hydrological Modeling and Water Resources

Albert-Ludwigs-University of Freiburg

Marvin Lorff

Deciphering the impact of climate and hydrology on recession-based discharge analysis

Examiner: JProf. Dr. Andreas Hartmann

Co-Examiner: Dr. Michael Stölzle

MSc-Thesis under the guidance of JProf. Dr. Andreas Hartmann

Freiburg i. Br., Mai 2020

Declaration of Authorship

I hereby declare and confirm that this thesis is entirely the result of my own original work. Where other sources of information have been used, they have been indicated as such and properly acknowledged. I further declare that this or similar work has not been submitted for credit elsewhere.

Freiburg i. Br., 20 Mai 2020

Marvin Lorff

Table of Contents

List of Figures

List of Tables

List of Figures in Appendix

List of Tables in Appendix

List of Abbreviations

AET	actual evapotranspiration
CoVP	coefficient of variation of precipitation
ECA	European Climate Assessment
ECA&D	European Climate Assessment and Dataset
HI	humidity index
IQR	inter quantile range
MAP	mean annual total precipitation
MAPET	mean annual total potential evapotransipiration
mNSE	modified Nash-Sutcliff-Efficientcy
PET	potential evapotranspiration
PSeas	precipitation seasonality
RA	recession analysis
RAM	recession analysis method
RC	recession constant
REM	recession extraction method
RR	recession rate
WMO	World Meteorological Organisation

List of Symbols

T_{mov30}	30-days moving average over mean daily temperature [°C]
$\bar{P_m}$	mean monthly total precipitation
$\bar{P_y}$	mean annual total precipitation
δS	Change in Storage $[mm * day^{-1}]$
δ	Sun shine declination angel $[radiant]$
a	Fraction of recharge to conduits reservoir $[mm]$
a	Recession constant, response time $[days]$
c	Recession constant $[days]$
$CFMAX$	Snow melt factor of HBV model $[mm/d/\check{r}C]$
CFR	Refreezing coefficient in HBV model [-]
CWH	Maximum water holding fraction of snow in HBV model [-]
dQ/dt	Time derivative of discharge $[mm * day^2]$
ET	Evapotranspiration $[mm * day^{-10}]$
ET_a	Actual Evapotranspiration $[mm * day^{-1}]$
ET_p	Potential Evapotranspiration $[mm * day^{-1}]$
h_0	Maximum soil water capacity $[mm]$
k	Recession rate [-]
k_c	Linear storage-outflow parameter of conduit reservoir $[days]$
k_m	Linear storage-outflow parameter of matrix reservoir$[days]$
lat	Latitude $[dec.degree]$
len	Length of the time series $[days]$
$mNSE$	modified Nash-Sutcliff-Efficiency
N	Average length of the month $[days]$
N	Average potential sun shine duration $[hr]$
P	Precipitation $[mm * day^{-10}]$
Q	Runoff $[mm * day^{-10}]$
Q_0	Runoff/Discharge at time 0 $[mmm * day^{-1}]$
R	Recharge to groundwater $[mm]$
RF	Refreezing water in HBV model $[mm/day]$

SCF	Snow fall correction factor of the HBV model [-]
T	Mean monthly temperature [řC]
t	Time [$days$]
TE	Thornthwaite's temperature efficiency index
TT	Threshold Temperature of HBV Model [řC]
V_C	Volume of conduit Reservoir [mm]
V_M	Volume of matrix reservoir [mm]
V_S	Volume of soil reservoir [mm]
P_m	Monthly precipitation sum
P_y	Annual precipitation sum

Acknowledgements

I would like to thank JProf. Andreas Hartmann for sharing the idea of this thesis with me and for the possibility to work on such an interesting research topic. Also I would like to thank Dr. Michael Stölzle for sharing his knowledge about recession analysis with me and providing advises on figure construction. I would like to thank Dr. Yuan Liu, for helping with the HBV snow routine parametrisation and thanks to Ass. Prof. Naomi Mazzilli for helping with data from the "Fontaine de Vaucluse" catchment.

Furthermore I am very grateful for Julian Hydgen who helped me some LaTex issues and especially grateful for Robin Schwämmle sharing his LaTex-template with other students.

Abstract

Recession analysis is a common and important tool for low flow analysis and prediction. While traditional baseflow recession analysis methods on observed hydrographs try to minimize the influence of quickflow, the true value of recession parameters is indeterminable. Recession parameters tend to be highly variable in time and space, yet they are assumed to reflect aquifer properties only. Previous studies tried to explain the variability of recession parameters among catchments and seasons with a climatic influence. This study aims to elucidate the influence of climate and hydrology on recession constants with a virtual experiment. Hydrograph recessions during baseflow conditions are generally a function of groundwater storage. In a mature karst aquifer there are two types of underground water storage: the conduits storage and the matrix storage. A simple two parallel storage model is used to incorporate these two groundwater reservoirs and to simulate the global response of a karst spring to rainfall events and snow melt. 814 climate records from weather stations in Europe (ECA data) are used as input for the simulation. Two common methods of linear recession analysis (Vogel and Kroll 1996; WMO 2008) are applied to the modeled karst discharge. Different parameter sets model varying degrees of karstification. The linear outflow parameter of the matrix reservoir(k_m), gives the expected value for the recession constant.

The results show that both hydrology and climate have a significant influence on recession constants. The deviation of WMO recession constants to the expected value and their variability are bigger when the conduit network is better connected and therefore draining faster. The deviation of Vogel & Kroll recession constants are behaving the opposite. The climate influence is significant on both recession analysis methods. Correlations are highest for mean annual precipitation and the coefficient of variation of precipitation.

Keywords: Recession analysis, Linear recession constant, Two parallel storage model, Climatic influence

Zusammenfassung

Rezessionsanalyse ist ein lange bekanntes und gebräuchliches Instrument für die Analyse und Vorhersage von Niedrigwasserabfluss. Während traditionelle Basisfluss-rezessionsanalysemethoden von beobachteten Ganglinien versuchen, den Einfluss der schnellen Abflusskomponte zu minimieren, bleibt der wahre Wert des Rezessionsparameter unbestimmbar. Rezessionsparameter neigen dazu, zeitlich und räumlich sehr variabel zu sein, jedoch geht man davon aus, dass sie nur die Eigenschaften des Aquifers widerspiegeln. In früheren Studien wurde versucht, die Variabilität der Rezessionsparameter zwischen Einzugsgebieten und Jahreszeiten mit klimatischem Einfluss zu erklären. Diese Studie zielt darauf ab, den Einfluss von Klima und Hydrologie auf Rezessionskonstanten mit einem virtuellen Experiment zu erklären. Rezessionen von Abflusskurven während Basisabflussbedingungen sind im Allgemeinen eine Funktion des Grundwasserspeichers. In einem ausgeprägten Karst-Aquifer gibt es zwei Arten der unterirdischen Wasserspeicherung: die Speicherung in den Karst Röhren und in der zerklüfteten Gesteinsmatrix. Ein einfaches Zwei-Parallel-Speichermodell wird verwendet, um diese beiden Grundwasserspeicher darzustellen und die globale Reaktion einer Karstquelle auf Niederschlagsereignisse und Schneeschmelze zu simulieren. 814 Klimadatensätze von Wetterstationen in Europa (ECA-Daten) werden als Input für die Simulation verwendet. Zwei gängige Methoden der Rezessionsanalyse (Vogel und Kroll 1996; WMO 2008) werden auf die modellierten Abflussganglinie angewendet. Verschiedene Modelparameter simulieren unterschiedliche Grade der Verkarstung. Der lineare Ausflussparameter des Matrixreservoirs (k_m) gibt den erwarteten Wert für die Rezessionskonstante an.

Die Ergebnisse zeigen, dass sowohl die Hydrologie als auch das Klima einen signifikanten Einfluss auf die Rezessionskonstanten haben. Die Abweichung der WMO-Rezessionskonstanten vom erwarteten Wert und ihre Variabilität sind größer, wenn das Karst-Röhrennetzwerk besser verbunden ist, d.h. schneller drainiert. Die Abweichungen der Vogel & Kroll-Rezessionskonstanten verhalten sich genau umgekehrt. Der Klimaeinfluss ist bei beiden Rezessionsanalysemethoden signifikant. Die Korrelationen sind für den mittleren Jahresniederschlag

und den Variationskoeffizienten des Niederschlags am höchsten.

Stichworte: Rezessionsanalyse, Lineare Rezessionskonstante, Zwei-Parallel-Speichermodell, Klimaeinfluss

1 Introduction

1.1 Introduction to Karst Hydrogeology and Karst Water Resources

In European countries karst is a common geological formation, since 21 % of the land subsurface of Europe is covered by karst (Chen et al. 2017). Karst is a special landscape and underground system that develops on carbonated rock. Characteristic to karst systems are sink holes (dolines), dry valleys and springs at the surface and a network of conduits and caves underground, where groundwater can move rapidly. Karst systems are formed due to rain water that dissolves the carbonate minerals (e.g. Calcite ($CaCO_3$)) over time. Rain water reacts with carbon dioxide from the atmosphere, creating carbonated acid (H_2CO_3). Infiltrating water accumulates more acid in the soil due to microbiological activity, before it reaches the carbonate bedrock. In geological timescales (tens of thousands of years) the acid dissolves the carbonate rock, according to the Equation 1.1 (Blume et al. 2010, S.40) leaving characteristic karst features.

$$CaCO_3 + H_2C0_3 \implies Ca^{+2} + 2HCO_3^- \tag{1.1}$$

Karst systems therefore have high spatial heterogeneity, because they have both a hardly permeable matrix where permeability ranges from $10^{-12}m/s$ to $10^{-6}m/s$ and conduit network with permeability of $10^{-1}m/s$ up to $10^{1}m/s$ (Borgomano et al. 2013). Karst springs are known for having relatively high discharge, as karst systems normally concentrate their discharge of a wide catchment area at a single drainage point, often at the boundary to no-karst terrains or at the lower end of the aquifer (Fiorillo 2014). Hence, they are particularly productive water sources. Around the world groundwater resources are the most important source of drinking and irrigation water. Karst water resources are substantial for water supply of humankind, since around 25% of the earth's

population depends at least partly on water resources from karst aquifers (Ford and Williams 2013). In a changing world, increasing population, rising contamination and dramatic change in climate conditions threatens water resources and require reliable estimations of utilizable karst water resources. Thus sustainable management of karst aquifers is therefore one key challenge for the future world (Hartmann et al. 2014). If temperature is increasing and precipitation is decreasing like in most climate change scenarios for Europe (Christensen and Christensen 2007), this will affect the groundwater levels and eventually will led to water scarcity and droughts in some regions. Observations on karst springs (measurements of their physical and chemical properties) are indispensable as well as modeling of the usable water resources when we want to achieve sustainable management of those aquifers and springs. Estimating water volumes of aquifers and their behavior during periods of low flow is especially crucial for predicting water scarcity.

1.2 Basics of Recession Analysis

Recession analysis (RA) on hydrographs is a common and valuable tool for hydrologists to study low flow behavior of streams and springs. Spring or stream hydrographs show the variation of discharge/runoff over time and represent the integrated hydraulic behavior of the aquifer respectively catchment. The recession curve is the declining part of the hydrograph. It contains valuable information about natural sources feeding the stream or spring and provides insights into the underlying aquifer. This information can be used to calibrate rainfall-runoff models by determining the storage outflow function, to predict discharge during low flow conditions (Tallaksen 1995) and to assess the effective storage capacity of the aquifers. It has also practical use for studying the anthropogenic impact on water resources and is crucial for water supply and waste water management, as well as for ecosystem sustainability (Dewandel et al. 2003; Smakhtin 2001; Tallaksen 1995). Integrating the recession curve provides an estimate of effective water storage, which means water available for drainage (Hall 1968).

Quantitative analyses of baseflow recession are widely used in hydrology and emerged from early studies of groundwater flow to the rivers (Boussinesq 1877) and from discharge analysis from karst springs (Maillet 1905). Hall (1968) wrote

the first review on baseflow recession analysis and defined baseflow as the component of flow that comes from groundwater storage or other delayed source. The hydrograph recession curve can be divided into two distinct sections: the "influenced" stage, where quick flow dominates and the "baseflow" stage when only the saturated zone discharges. The baseflow recession is the most representative feature of an aquifer's global response because it is less influenced by the temporal and spatial variations of infiltration (Kovács et al. 2005). By fitting analytical models to the baseflow recession curve the storage-outflow relation of the aquifer can be assessed, and characteristic recession parameters can be obtained. One common recession parameter is the recession constant (RC).

Fundamental to baseflow recession analysis on streamflow or discharge hydrographs, is the equation from Boussinesq (1877). It describes the outflow from a large unconfined aquifer into a stream under idealized conditions (no recharge, no leakage and no evapotranspiration). The linearized Boussinesq-equation or its alternate form (1.3) is regarded as the origin of the recession models and was continuously developed further in the following years (Hall 1968).

$$Q_t = Q_0 * e^{\frac{-t}{C}} \tag{1.2}$$

$$Q_t = Q_0 * k^t \tag{1.3}$$

Where Q_t is discharge at time t and Q_0 is the initial discharge at $t = 0$. The depletion factor, or recession rate (RR), is k (dimensionless) and is commonly used to define the extent of the recession and ranges from 0 to 1, normally > 0.7 (Tallaksen 1995). Typical ranges of k for various runoff components are: overland runoff $k = 0.2 - 0.8$, interflow $(0.7 - 0.9)$, and groundwater flow $(0.93 - 0.995)$ (Nathan and McMahon 1990). However in practice those runoff components always overlap and therefore are hard to separate. C in Equation 1.2 is the RC and describes the time elapsed between any discharge Q and Q/e on the recession curve (Tallaksen 1995). The reciprocal value of RC is known as the recession coefficient.

Since the beginning of recession analysis almost 150 years ago, a great variety of recession analysis method (RAM) have been developed, which makes it difficult to compare results from different studies and authors with each other. However, most modern studies use slightly different adaptions of the approach

from Brutsaert and Nieber (1977).

In times of no or very little precipitation the falling part of the hydrograph is the recession curve, illustrated in Figure 1.1. The recession period continues as long as the discharge is decreasing. Recession segments are extracted from the hydrograph depending on the recession extraction method (REM) (see examples in subsection 3.7.1) and can be analysed collectively or individually. By plotting dQ/dt versus Q on a semi-log scale, a linear model can be fitted through those points (see examples in subsection 3.7.2). Other approaches, which derive linear recession parameters from a "master recession curve" (MRC) have been used traditionally (Barnes 1939) and are still used by some researchers nowadays (Fatchurohman et al. 2018; Malík and Vojtková 2012; WMO 2008). The linear recession rate can be obtained by fitting a linear model to Q_t versus Q_{t-1}, which describes the slope of the MRC. However, usually analytical solutions are used to develop mathematical models that describe the recession curve (Hall 1968).

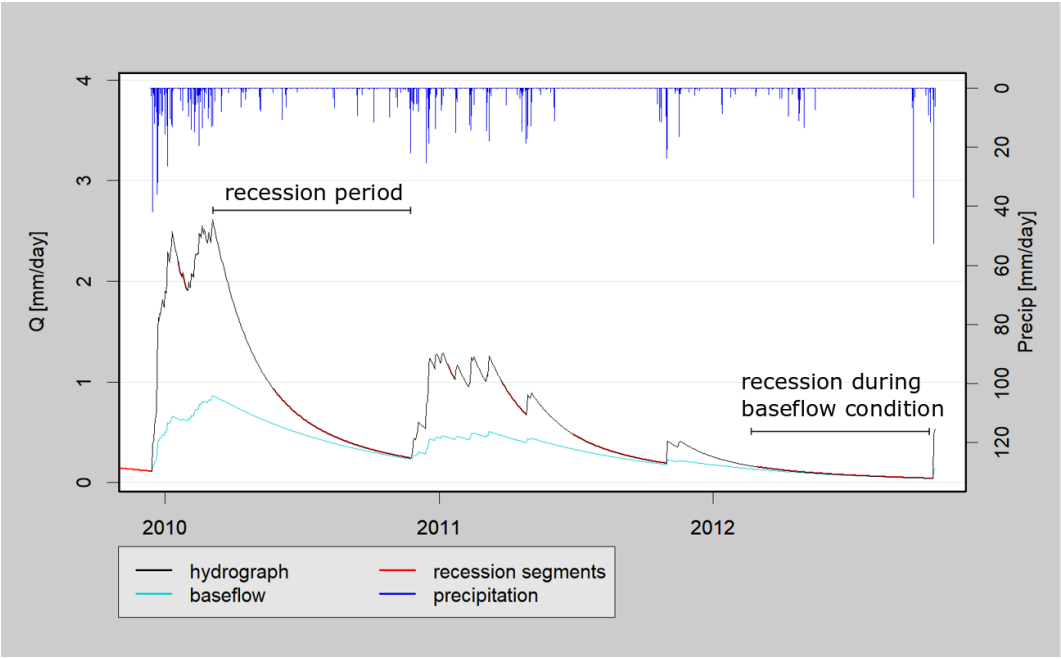

Figure 1.1: Precipitation, modeled hydrograph and modeled baseflow during the years 2010 - 2013, applied identification to recession curve, period and segments and recession during baseflow conditions

The RC together with other recession parameters are assumed to be characteristic for the investigated catchment. Recession analysts link those recession characteristics to the catchment's hydraulic and geologic properties (Hall 1968; Price et al. 2011). Some studies have tried to predict recession characteristics

with catchment features such as climatic and topographical attributes (Beck et al. 2013). Bogaart et al. (2016) said that recession parameters are strongly related to landscape, soil and climate. Furthermore factors that control recessions rates are watershed geomorphology (Price et al. 2011; Smakhtin 2001) and evapotranspiration losses (Federer 1973; Weisman 1977). However regionalization and prediction in ungauged catchments is still challenging (Krakauer and Temimi 2011). Other studies have analysed global patterns of recession parameters (Berghuijs et al. 2016). Recession analysis is also used to investigate human interference on groundwater resources (Bogaart et al. 2016; Wang and Cai 2009).

1.3 Storage-Outflow Relations

River flow can be considered as an interaction of different streamflow components from various sources. Conceptually the river catchment can be interpreted as an arrangement of linked reservoirs, in series or parallel, where each of them has its own recharge, storage capacity and discharge function (Smakhtin 2001). During the recession period, water which is stored in the catchment is continuously drained and no recharge is filling up the storage. Thus the stream flow decreases as well as the water volumes of the reservoirs which store the water in several units.

Storage depletion and discharge are related by the water balance equation, the most fundamental equation in hydrology:

$$P = Q + ET + \delta S \tag{1.4}$$

where P refers to precipitation, ET to Evapotranspiration, Q to discharge and δS to the change in storage for the investigated time interval.

Each hypothetical water storage unit in the catchment (e.g. interception storage, surface storage, soil storage, aquifer storage) has its own storage volume and respective runoff component, such as throughfall, overland flow, subsurface flow and groundwater flow. The combination of all those draining storages result in the hydraulic response to precipitation events, often referred to as the global response of the stream or aquifer (Kovács et al. 2005). Each storage unit also

has its own recession rate, which describes its runoff behavior. In the beginning the streamflow recession rate is quite steep because all the quick responding elements control the streamflow e.g. overland flow. When only delayed sources (groundwater, lakes and glaciers) contribute to the spring or river flow this is called baseflow (Hall 1968). Typically recession analysis tries to capture the more stable part of the hydrograph that is only influenced by baseflow, also referred to as baseflow recession.

The main idea behind recession analysis (RA) is the direct relationship between storage depletion and discharge. During baseflow recession, input i.e. precipitation is zero or negligibly small (dry period) and evapotranspiration as well as groundwater extraction from the aquifer is assumed to be negligible (Moor 1996). Under these conditions, stream flow is only a function of catchment storage, and thus the water balance equation reduces to the expression of Equation 1.5, which expresses discharge Q as a function of storage change over time (dS/dt). This is also referred to as the storage-outflow relation.

$$dS/dt = -Q \tag{1.5}$$

Numerous equations evolved to describe different types of recession from various storage units. Table 1.1 gives an overview of five storage units, their recession models and storage-outflow relations.

The storage-outflow relation is another way of describing the recession curve. Whereas equation Equation 1.3 is an implicit calculation, storage-outflow function is a recursive calculation. It describes the discharge from a conceptual storage at a given time step, where the discharge is only a function of storage volume, in the case of no input and neglectable evapotranspiration to/from the storage.

The most common method for characterising the relation between groundwater storage and baseflow was introduced by Brutsaert and Nieber (1977).

$$Q_t = a * S_t^n \tag{1.6}$$

Equation 1.6 assumes a power law relationship between aquifer storage S_t and baseflow discharge Q_t at time t and is able to describe exponential storage-outflow relations ($n \neq 1$) as well as linear storage outflow relations ($n = 1$) with a linear recession constant a. Often, however, linear storage-outflow relations

Table 1.1: Table of various storage-outflow models used in the field of recession analysis, adapted from Brodie and Hostetler (2005)

Conceptual model	Storage-outflow relation	Recession function	Storage types	Source and comment
Linear model	$Q = k * S$	$Q = Q_0 * e^{-ct}$	General storage	Boussinesq (1877) linearised Depuit-Boussinesq equation.
Exponential reservoir	$Q = Q_B * e^{-\phi SD}$	$Q = Q_0/(1 + \phi Q_0 t)$	Throughflow in soil	Hydraulic conductivity assumed to exponentially decrease with depth (Beven and Kirkby 1979).
Power-law reservoir	$Q = \alpha S^n$	$Q = Q_0(1 + \mu t)^p$ $p = n/(1 - n)$ $\mu = \alpha^{1/n}(n-1)Q_0^{\beta-1} * n$	Springs and unconfined aquifers	Hall(1968); Brutseart and Nieber (1977), Recession modelled using $p \approx 1.67$ (Wittenberg 1994)
Two parallel linear reservoirs	$Q = k_1 S_1 + k_2 S_2$	$Q = Q_1 * e_1^{-k} * t$ $+ Q_2 * e_2^{-k} * t$	Independent aquifers	Barnes (1939)
Cavern storage		$Q = \alpha_1 - \alpha_2 * t$	Underground caverns in karst terrain	Griffiths and Clausen (1997)

can not adequately represent recession flow over a wide range.

The Brutsaert-Nieber-Approach estimates the parameters of this equation by plotting dQ/dt against Q, where Q is the discharge during baseflow conditions (see subsection 3.7.2 for an example). It has the advantage of being time independent, and therefore not only makes different recession segments comparable to each other but also makes recession plots from different catchments easier to compare. Either individual recession segments, seasons or all data pairs can be visualized and used to estimate recession parameters. Most modern methods are based on this concept dQ/dt versus Q. Other methods

obtain

Equation 1.6 showing the relationship between aquifer storage and baseflow discharge from Brutsaert and Nieber (1977) and is combined with the reduced form of the water balance equation during baseflow $\delta S = -Q$ when input P is zero and ET negligibly small compared to Q (Kirchner 2009). This leads to Equation 1.7.

$$dQ/dt = -aQ^b \tag{1.7}$$

With this differential equation, a variety of hydraulic aquifer properties can be described and their recession behavior analysed. Under the constraint of $b = 1$, the storage acts as a linear reservoir with a fixed storage-outflow function. Horton (1933) provided the first non linear relationship and Wittenberg (1999) has shown that the storage outflow relationship from an unconfined aquifer tends to be non linear, with $b = 1.5$. However, in this study we focus more on linear storage outflow relationships, rather than exploring more regarding the non linear outflow model approach.

1.4 Karst Spring Recession Analysis

Karst systems are highly heterogeneous and anisotropic (Bakalowicz 2005), because of the duality of matrix and conduit. When investigating groundwater flow in karst systems, this heterogeneity is represented by the concept of a highly conductive karst conduits network - with water moving freely (quick-flow), embedded in a low permeability fissured rock matrix - where water only drains very diffusively (baseflow), differences in permeability are in the range of 10^5 and 10^{10}.

The whole recession, composed of the *influenced-stage* and *baseflow stage*, can be seen as the interaction of two independently draining storages units: a) the fast draining network of karst conduits and b) the water stored in fissured matrix of the rock being slowly drained. (Fiorillo 2014). When plotting the recession limbs on a semi-log scale, the drainage from the karst matrix can be identified by its constant slope. The slope of the recession curve depends on the degree of karstification. Whereas karst springs with a very pronounced conduit network tend to have a fast recession, meaning the water in the aquifer

drains quickly from the storage, only slightly karstified fissures drain slowly and holding water for a long time. Therefore, recession curves have steeper slopes in strongly karstified systems and, respectively, are flat-angled in less karstified areas (Fiorillo 2014). The shape of the recession curve is controlled by the outflow parameter of the karst conduits storage and of the limestone matrix reservoir. During baseflow recession only the saturated zone is involved whereas the vadose zone, i.e. epikarst, only contributes during early stage of the recession i.e. *influenced-stage* (Fiorillo 2014). Kovács et al. (2005) also stated that during the baseflow recession the drainage of the flow systems should be influenced by the parameters of the karst matrix alone and not by the parameters of the conduit system. The baseflow recession behavior of karst systems can be described by the same exponential equation which was used by Maillet (1905). It assumes the drainage of a single reservoir and is generally interpreted as drainage from the limestone matrix (Kovács et al. 2005). Bagaric (1978) (cited by Kovács et al. (2005)) provided an analytical solution for diffusive flux from a one dimensional block, with a fixed boundary condition at one edge and no infiltration. The discharge from this block can be expressed by the following equation:

$$Q(t) = Q_0 * \exp\left(-t * \frac{2T}{SL^2}\right) \tag{1.8}$$

where $Q(t)$ is discharge at time t, Q_0 is initial discharge, T represents hydraulic transmissivity [m²/time], S the sorativity [-] and L is the length of the block [m]. In this case the recession constant can be calculated as $a = 2T/SL^2$. The same has been done for the diffuse flux from a 2D block and for other special cases (Fiorillo 2014; Kovács et al. 2005). A vast variety of recession models have been evolved for various karst aquifer geometries (Dewandel et al. 2003). Fiorillo (2014) gives an overview on empirical and physical based models that can describe recession curves. Jeannin and Sauter (1998) describe three lumped recession models and methods to characterise their hydrodynamics by the model parameters. However, though most complex models could achieve a good fit to recession curves, model parameters are often difficult to interpret or prove accurate.

Characterising karst aquifers by the shape of their hydrograph was developed early and is still common practice (Bonacci 1993; Schmidt et al. 2014; White

2002). Pronounced peaks indicate a good connection of the conduits (Fiorillo 2014) and flashiness is a measurement for the differences between Q_{max} and Q_{min}. Also a definition of the degree of karstification was introduced by Rashed (2012) using baseflow separation and flashiness of karst spring hydrographs. Another classification of the karst springs into 10 classes of karstification based on the "master recession curve" was developed by Malík and Vojtková (2012).

Karst aquifers are also characterised by hydraulic parameters acquired by recession analysis (**Mangin.1975**). Kovács et al. (2005) suggest a conceptual model where the karst aquifer consists of a rectangular shape with certain spatial extent and a regular distributed network of high-conductivity karst conduits embedded in the low-permeability matrix. The model is parameterized with the hydraulic conductivity of the matrix and conduits and the conduits spacing.

The general opinion was that the recession constant of karst system exclusively depended on the hydraulic parameters of the low-permeability matrix and neglected the influence of the conduit network. However Kovács et al. (2005) found out that this is only true for mature karst systems and first provided a mathematical term for the influence of the conduits parameter on baseflow recession analysis. Sensitivity analysis of karst models predicted higher baseflow recession coefficients as a consequence of an increasing conduit network conductivity (Eisenlohr et al. 1997).

The outflow from a karst system is often a single spring and the hydrograph of this spring allows an integral characteri szation of the the whole catchment (Jeannin and Sauter 1998). Therefore, most models which describe the recession curve of karst systems are lumped models and few models consider the spatial heterogeneity of the aquifer. Recession parameters are considered only to represent the aquifer properties. Recession analysis of springs is generally performed without considering recharge processes, because the main intent is to obtain the drainage behavior of aquifers and to predict discharges under drought. Thus climatic characteristics, e.g. the type and time-space distribution of the precipitation receive no consideration (Fiorillo 2014). However some authors are discordant (Beck et al. 2013; Hall 1968; Jachens et al. 2020; Jeannin and Sauter 1998; Peña-Arancibia et al. 2010; Tallaksen 1989).

2 Aim of the Study

2.1 Research Gap

The basic assumption of recession analysis is that the shape of the recession curve and the recession parameters obtained from them only depend on physical aquifer and basin properties, such as landscape, land cover, soil, geology, hydraulic conductivity, aquifer thickness and aquifer general geometry, watershed topology and topographic attributes (Bogaart et al. 2016; Brutsaert and Nieber 1977; Dewandel et al. 2003; Karlsen et al. 2019; Peña-Arancibia et al. 2010; van Dijk 2010). Analyzing recession segments collectivly, numerous studies have found very high variability in recession parameters from one catchment (temporal variability) which could not be explained by differing aquifer properties (Dewandel et al. 2003; Shaw and Riha 2012; Tallaksen 1989, 1995; van Dijk 2010). However, in recent literature there has been a shift toward analyzing individual recessions segments rather than all segments at once to estimate recession parameters more accuartly (Basso et al. 2015; Karlsen et al. 2019; Santos et al. 2019). The variability of recession parameters might be on the one hand due to the circumstances that the limiting factor when analyzing hydrograph recession is the quality of low flow data. Recession analysis methods can only be exact when being applied to a high quality low flow data (Tallaksen 1995) Also a certain quantity of discharge data is needed, Perzyna (1993) found that a minimum of 10 years of data was necessary to provide reliable estimates of recession parameters for one catchment. On the other hand the variability accrues due to the fact that research using different recession analysis methods can hardly be compared to each other, despite the development of computer algorithms that eliminate the subjective elements of recession analysis. Stoelzle et al. (2013) proved that differing recession extraction methods and recession model fitting methods lead to completely different recession parameters. Analyzing 20 meso scale catchment with a combination of 3 recession extraction method and 3 recession model parametrisation methods (9 different approaches) concluded that

the differences between recession analysis method are bigger than difference between the catchments. The recession time in days, similar to the recession constant, obtained by different methods span from several days to nearly a year.

Although these are reasons for the variability of recession parameters, one more driver for the variability could be the effect of climate. Against the general opinion, some authors suppose that the amount, type and time-space distribution of precipitation influences the recession parameters and therefore cannot be negligible. Hall (1968) doubted that recession parameters e.g. the storage/flow ratio or response time - as he called the ratio of V/Q or $\delta V/\delta Q$ are constants properties of the drainage basin. He challenged the assumption that the response time is a constant over the several years when meteorologic (hydrologic and geologic) factors are not remain constant. Jeannin and Sauter (1998) stated that rainfall frequency could have a significant influence on recession parameters because it determines the selection and length of recession segments from the hydrograph. Dewandel et al. (2003) also said that climate and seasons play an important role for the shape of the recession curve and Grasso and Jeannin (1998) found that recession parameter could also be dependent on the recharge type. Despite the fact that many authors claimed the influence of climate on spring or stream recessions, none of them really investigated the effect of climate alone on recession parameters (Beck et al. 2013; Peña-Arancibia et al. 2010). When studying recession parameters of observed streamflow data the influence of climate mixes with other properties of the catchment.

2.2 Hypothesis

There are reasons to presume that the variability of the recession parameters is influenced by a component that is variable in space and time. Because the recession segments are always separated from each other by rainfall or snow melting events it might be the type and distribution of precipitation. There are inter-annual recession events during the wet season, which often last no longer than several days or weeks, but also seasonal recession events, lasting months. During the dry season, precipitation is often significantly less or is directly evaporated without contributing to groundwater recharge. Hence long summer recessions evolve from that.

This can also be adumbrated when looking at figue 1.1.The plot shows three

years of rainfall events and the modeled hydraulic response in Malaga, Spain. The first year was a very wet year (precipitation amount 1207 mm) compared with the annual mean precipitation of 500 mm. The second year was an average dry year and the third year, with annual rainfall of 250 mm, is significantly dryer than previous years. During the first two years, the recession curve covers a wide span of discharge values, but during the dry year the recession line meets the baseflow very well. When this is the case the recession curve and even more so the selected recession segments from the recession analysis method only represent the baseflow recession and are less influenced by quickflow drainage of conduit storage.

So when we want to look at baseflow recessions and compare different catchments, years or seasons with one another, we might have to take into account the fact that precipitation events influence the recession behavior. This leads to the hypothesis of this study:

"Recession parameters not only reflect the hydrologic signal but mix together with a climatic signal."

To be more precise, i will try to answer the following questions in this study:

a) Can we detect patterns in the variability of recession parameters?

b) How do the variability and the bias of recession parameters obtained from different recession analysis methods behave?

c) Is there a dependency of climate indices and recession parameters?

d) If so, how does this dependency change with between different hydraulic properties of the aquifer?

2.3 Research Objectives

The objective of this thesis is to investigate this hypothesis by using a virtual modeling experiment. The following steps are therefore mandatory:

- Get daily climate data (precipitation and evapotranspiration) from a wide range of climate conditions
- Develop a two parallel storage rainfall-runoff model with linear outflow functions to calculate discharge of an ensemble of synthetic karst systems with varying degrees of karstification.
- Apply different recession analysis methods to simulated discharge time

series and obtain recession constants from a linear outflow model.

- Compare the deviation of the obtained recession constants to climatic indices and karstification degrees.

3 Methodology

A virtual experiment is conducted to address the research objectives of this study. Firstly a variety of input data for the model is needed. The data from European Climate Assessment (ECA) covers the greater area of Europe and includes precipitation and evapotranspiration measures on a daily resolution. Potential evapotranspiration (PET) is calculated with a temperature based approach. This data not only feeds into the model but is also used to calculate climatic indices, such as mean annual PET, precipitation seasonality as well as mean annual precipitation sums to characterise different climate conditions.

The hydrological model, that was devolved in this work uses a snow routine that was inherited from the HBV-model and a simple soil routine where evaporation takes place. Infiltration water is then divided into two reservoirs, one which represents karst conduit storage and one which represents the matrix storage. Different parameter settings of those two parallel reservoirs represent artificial karst systems with a varying degree of karstification e.g. more or less developed system of karst conduits. The simulated hydrograph is computed as the linear outflow from both of those storage units.

Next, two different RAM, one introduced by the World Meteorological Organisation (WMO), (WMO 2008) and one common approach based on the work of Vogel and Kroll (1992) were used on the simulated hydrograph to calculate specific recession constants for every input data set and every artificial karst system.

Finally the computed recession constants were compared with the linear outflow parameter of the matrix reservoir in the model. Thus we can not only determine which methods performs better, but also compare the deviation from the expected recession constant to climatic attributes and model parameters, representing geomorphological attributes of the karst system.

All computation and modeling in this study was performed in R, a software for statistical computing with the help of some additional packages. A full list of packages that there used for this study and also all R-scripts are provided in the supplementary materials.

3.1 Input Data

Daily observations of mean air temperature and total precipitation were gathered by the European Climate Assessment and Dataset (ECA&D) project. This dataset is open access and available on the ECA&D website under https://www.ecad.eu/dailydata/ (last visited 11.09.2019). It contains observations from weather-stations from the European region. The data was subject to quality control and was tested on climate trends by (Klein Tank et al. 2002). The ECA&D also provides a table with meta-information for every weather station, including the geo-information (latitude, longitude and height) and the country code. Other information such as the length of the time series and several climate indices were added to the table during the work of this study. The full table with all information regarding the weather stations used in this study can be found in the supplementary materials.

The input data holds 13506 time series of precipitation and 3549 time series of temperature data, however only a selection of those data sets were used in this study. The following criteria had to be fulfilled for the stations to be included:

- Temperature and precipitation observations available for the same station and for the same period of time (3306 Stations).
- Observations comprise the period from 01.01.1999 until 01.01.2018.
- Stations within the spatial extent of 35° – 75° latitude and -10° – 40° longitude.
- Since the model needs continuous input, stations were only included when there are no missing values in the precipitation time series (see section 3.2 to read about the handling of missing values in temperature time series).

Figure 3.1 shows a map of all 814 stations that were used in this study.

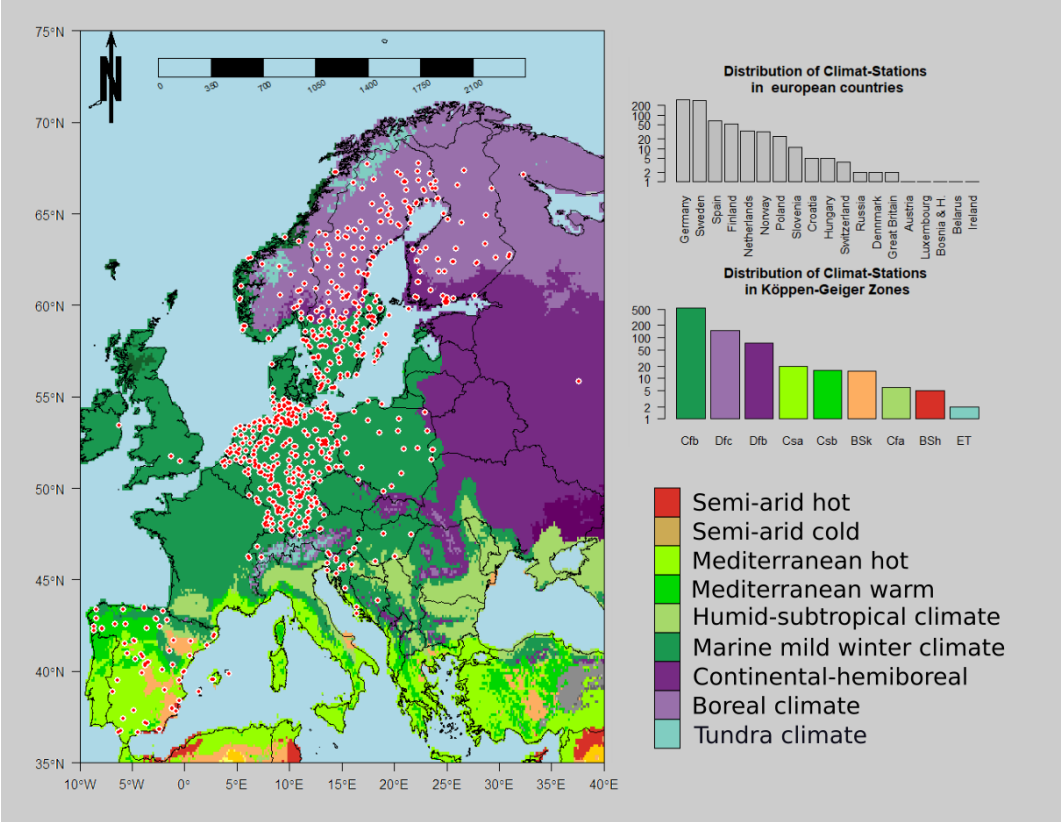

Figure 3.1: Location of weather-stations included from the ECA climate data, visualized with Köppen-Geiger climate zones, additionally log scale barplots of the distribution of stations in Köppen-Geiger climate zones and distribution of stations in countries.

Some data processing was performed before continuing to work with temperature and precipitation data:

- Values in temperature of -9999 were replaced by NA (missing value).
- Missing values in temperature time series were replaced by an average temperature of the given day of the year.
- Values in temperature and precipitation were corrected by a factor of 0.1 to transform units to °C and mm respectively.
- Geo-coordinates of weather-stations were transformed to decimal degrees.

3.2 Daily Potential Evapotranspiration

The temperature data itself is only required as an input for the HBV model, but it is important that the hydrological model takes evapotranspiration into

account, since the water has to pass through a soil storage before contributing to the aquifer recharge. Therefore a simple approach (Thornthwaite 1948) was used to calculate potential evapotranspiration (PET) as an input to the model. Based on the input of daily values of mean air temperature and the latitude of the weather-station, daily PET values were calculated using a modified Thornthwaite-equation.

Originally developed by Thornthwaite (1948), the Thornthwaite-equation was developed to rationally classify climate conditions around the world. Together with the Hargreaves-equation and the Pennman-Monteith-equation, they are the most common tools to calculate PET. However, the Thornthwaite-equation has the advantage of needing the least input (monthly mean temperatures and geographic latitude) to estimate monthly PET. For the R-package "SPEI" (Calculation of the Standardized Precipitation-Evapotranspiration-Index), the Thornthwaite-equation was translated in a ready-to-used R-function (Vicente-Serrano et al. 2010).

For the aim of this work the thornthwait-function in SPEI was rewritten in R to calculate **daily** instead of **monthly** PET values (Equation 3.1). PET effects the recession curve only indirect because the evaporation takes place from the soil reservoir and not the groundwater storage. However, it influences the duration of the (summer) recession because it empties the soil storage to a degree before the next rainfall event. When the maximum soil water storage increases this effect is getting bigger.

$$ET_p = 16 * \left(\frac{10T_{mov30}}{TE}\right)^a * \frac{N}{365} \tag{3.1}$$

ET_p is potential evapotranspiration and can be calculated with the polynomial a (Equation 3.2) and with TE, the Thornthwaite's temperature efficiency index. Equation 3.3 uses a 30-day moving average (T_{mov30}) over the daily mean temperature. If the moving average would fall below zero it is set to zero. N is the average potential sunshine duration (Equation 3.4).

$$a = 0.0000000675(TE)^3 - 0.0000771(TE)^2 + 0.01792TE + 0.49239 \tag{3.2}$$

$$TE = \sum (T_{mov30}/5)^{1.514} * \frac{12}{len} \tag{3.3}$$

$$N = \frac{24}{\pi} * \arccos(\delta - \tan\Big(\frac{lat}{57.2957795}\Big)) \tag{3.4}$$

Instead of monthly mean temperatures it uses the 30-day moving average on temperature to calculate the modified Thornthwaite's temperature efficiency index. len is the length of the time series. To calculate the average sun shine duration N, the solar declination angle δ is calculated as a function of the day in the year and lat which is the geographic latitude of the location on earth.

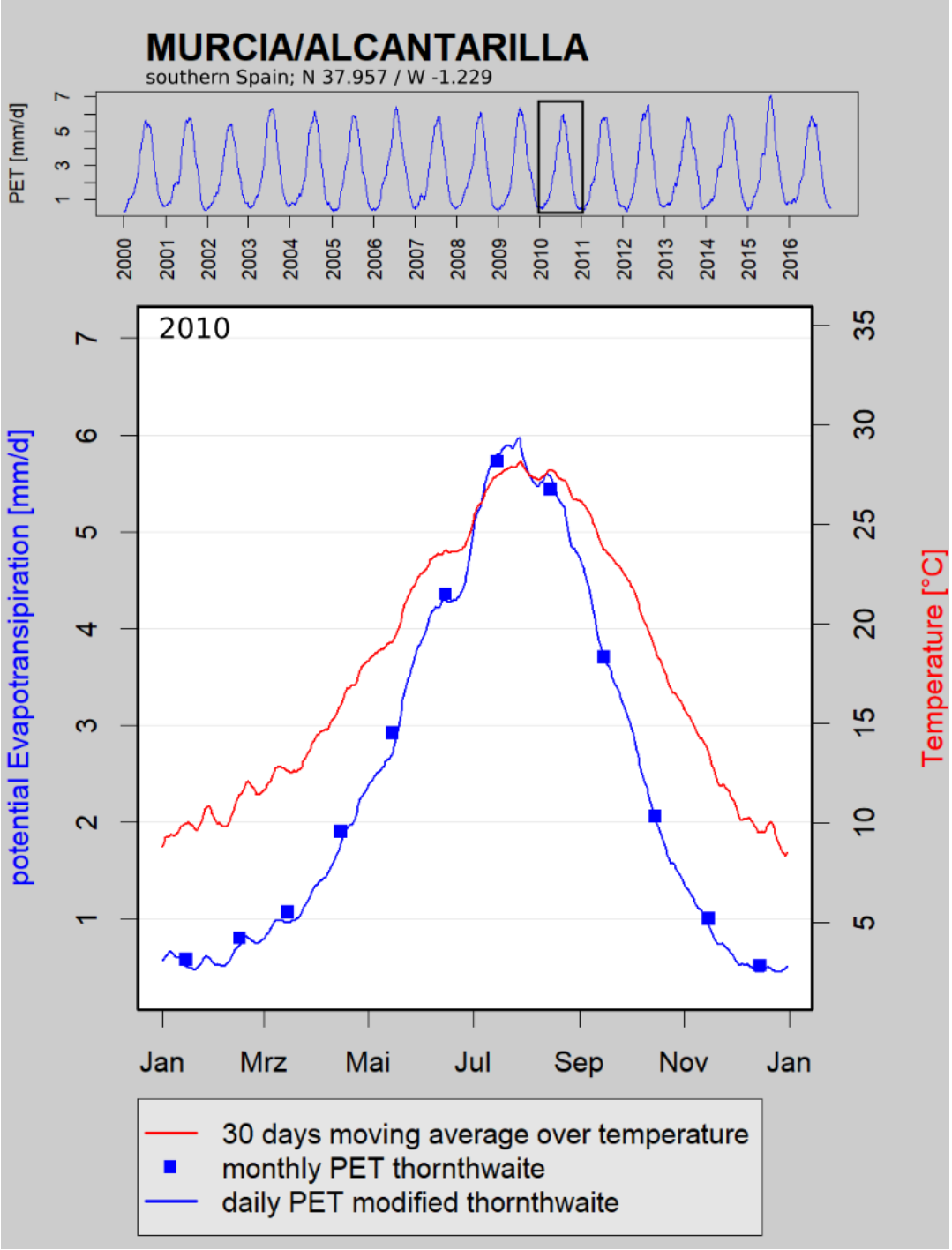

Figure 3.2: Comparison of the original Thornthwaite approach (monthly PET in blue squares) and the modified Thornthwaite-equations which calculates daily PET values (blue line) and is based on a 30-days moving average function over the temperature time series (red line) in the example year 2010 in Murcia, Spain

Figure 3.2 shows a comparison between the original Thornthwaite function from the R-package SPEI (Vicente-Serrano et al. 2010) and the modified version.

Mean monthly PET values divided by the number of days of each month were consistent with those daily PET values which were computed by the modified Thornthwaite function shown here as an example for Murica 2010.

3.3 Climate Indices

On the basis of the ECA&D data and the estimated PET, climate indices were calculated for every weather station. Table 3.1 shows an overview of climate indices included in the virtual experiment. They are later used to identify the influence of climate on the RCs.

Table 3.1: Table of climate indices

Climate Index	Abbr. [unit]	Source
Mean annual temperature	MAT [°C]	
Mean annual total precipitation	MAP [mm/year]	
Precipitation seasonality	PS [-]	Walsh and Lawler (1981)
Coefficient of variation in precipitation	MCVP [-]	
Mean annual snow cover	MASC [days/yearr]	
Mean annual total potential evapotranspiration	MAPET [mm/yearr]	
Humidity index	HI [-]	Hijmans et al. (2005)

There is only one index based on temperature (MAT) and two based on evapotranspiration data: MAPET and the HI. Four based on precipitation: MAP, PSeas CVP, MASC. Various other climate indices were considered but not included in the analysis, mostly due to the fact that there are based on the same input and strongly correlated with other climate indices.

Mean annual total precipitation was defined as the sum of rainfall and the assumed water equivalent of snowfall for a given year. Annual snow cover was defined as the sum of days with snow cover during the year and was calculated

with the help of the output from the HBV snow routine model (see subsection 3.4.1). The mean annual total potential evapotransipiration (MAPET) is the average of annual daily potential evpotraspiration sums, based on the modified Thronthwaite-equation. The humidity index (HI), also known as aridity index, is calculated as the quotient of mean annual total precipitation (MAP) and MAPET as suggested by UNEP (1992). The coefficient of variation of precipitation (CoVP) is defined as the ratio of the standard deviation of precipitation to the mean precipitation. The precipitation seasonality (PSeas) is a measure of the precipitation regime. It can take values from zero to about 1.2. Small values of PSeas indicate that precipitation is evenly spread over the year and bigger values show a more pronounced dry or wet season (Walsh and Lawler 1981) (as seen in Table 3.2). Its is defined as the sum of the absolute difference of mean monthly precipitation and the overall monthly mean $\bar{P_m}$ divided by the mean annual precipitation P_y in Equation 3.5.

$$\bar{PS} = \frac{1}{P_y} \sum_{n=1}^{12} \left| \bar{m_n} - \frac{\bar{P_m}}{12} \right| \tag{3.5}$$

Table 3.2: Table of precipitation regime classification by precipitation seasonality

Precipitation regime	Precipitation seasonality
very equable	≤ 0.19
equable with a definite wetter season	$0.20 - 0.39$
rather seasonal with short dry season	$0.40 - 0.59$
seasonal precipitation regime	$0.6 - 0.79$
seasonal with longer dry period	$0.8 - 0.99$
most precipitation 3 months or less	$1 - 1.19$
extreme, almost all precip. in 1 or 2 months	≥ 1.2

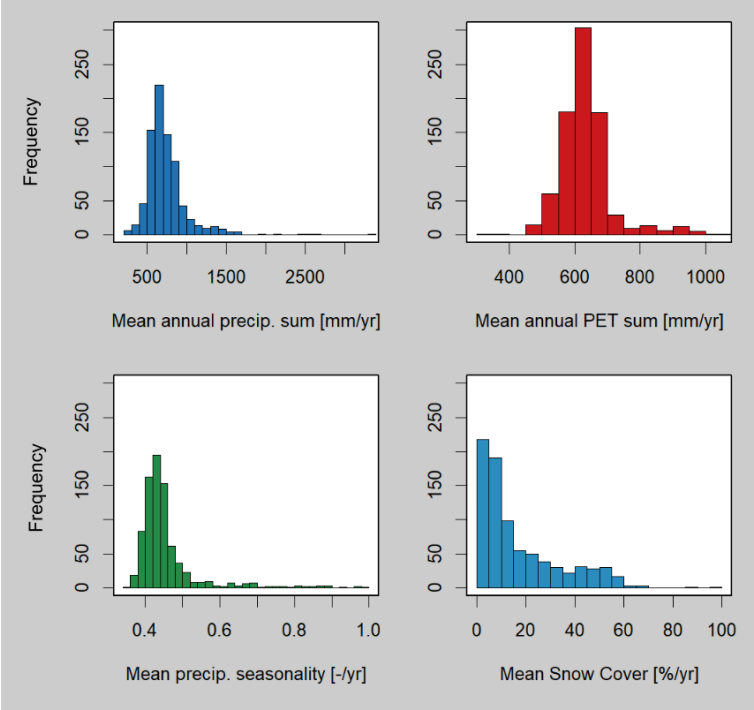

Figure 3.3: Histogram of the distribution of climate indices among selected weather stations in Europe

Figure 3.3 shows the distribution of climate indices among the 814 climate stations. These climate indices characterise the climate conditions in a sophisticated way. Thus the weather stations are not equally distributed around Europe, mostly central Europe (Germany) and Scandinavia are present, where marine and humid climate is mostly abundant. To summarise all weather stations, the climate condition can be characterised with an average temperature of 8.2 °C and an average annual total precipitation of around 680 mm, ranging from 202 mm up to 3312 mm, and inter quantile range (IQR) from 600 mm up to 820 mm. PS is narrowly distributed around a mean of 0.43 (sd = 0.087) but extreme values can be as high as 1. MAPET is ranges from 300 mm to 1050 mm with a median of around 630 mm and the IQR of only 45 mm, that is skrewed to the left. MASC is about 10 days on average but the median of 16 days and the maximum of 100 days indicate that some stations show much more snow cover throughout the year.

Based on their geographic location, each weather station was also assigned to their Köppen-Geiger climate zone (Kottek et al. 2006). A R-script provided by the Central Institute for Meteorology and Geophysics of Vienna, Austria was used to classify the weather stations into the Köppen-Geiger Zones. This R-

Code is freely available under http://koeppen-geiger.vu-wien.ac.at/present.htm (last visited 27.03.2020) and is also attached in the supplementary materials of this work. Figure 3.1 gives the distribution of the climate stations in Köppen-Geiger climate zones.

3.4 Hydrological Model

A lumped precipitation-discharge model was designed to calculate karst spring discharge. Lumped models can conceptualize physical karst processes that generate discharge at the scale of the whole karst system. Their benefits are lower data requirement, but they may also be limited in their prediction potential. Too few parameters often result in a low degree of process representation, whereas too many parameters often result in equifinality (insensitive parameters and many possible sets of parameters) and unrealistic calibration results.

All calculations of the model were performed on a daily bases. Daily values of precipitation, temperature and PET are required as input data. The model code can be inspected in the supplementary materials of this study.

3.4.1 HBV Snow Routine

The originally designed two parallel storage model misses out on an important runoff generating process, which is the accumulation and melting of snow. To compromise for this effect, a simple day-degree approach was used. The ECA&D data of precipitation and temperature was fed to the HBV snow routine model to simulate effective precipitation as the combination of melt water and precipitation (Seibert and Vis 2012).

The HBV model distinguishes precipitation between snowfall and rainfall. During all time steps, when the temperature falls below a certain threshold temperature (TT [°C]), normally around 0°C, precipitation is considered to fall as snow and is multiplied by a snowfall correction factor (SCF [-]). This factor adjusts for systematic errors in snowfall measurements and evapotranspiration from the snow pack. For the melting process of the snow cover, the HBV model uses a simple day-degree approach with the factor $CFMAX$ [mm/d/°C]. Equation 3.6 gives the melt water (M [mm]) controlled by the temperature T

[°C] at the time t.

$$M = CFMAX * (T(t) - TT) \tag{3.6}$$

Melt water and rainfall can be retained by the snowpack until it exceeds a threshold fraction CWH [-]. When temperature falls below TT [°C], water within the snowpack freezes again. The amount of freezing water RF [mm/day] is calculated by the model with the refreezing coefficient CFR[-] in Equation 3.7.

$$R = \text{CFR} * CFMAX * (TT - T(t)) \tag{3.7}$$

Eventually the effective precipitation (sum of rainfall and snow melt) [mm/-day] is used as the input for the soil routine, explained in the next chapter. A more detailed look on th HBV model is provided by (Seibert and Vis 2012).

3.4.2 Soil Routine

The soil routine consists of a soil-reservoir with a Volume (V) at time step t, that is filled by effective precipitation (P) depending on the input precipitation time series and the level of the reservoir in the times step before V_{t-1}. From this reservoir actual actual evapotranspiration (AET) takes place if there is water available. The soil routine has only one parameter h_0 which is the maximum soil water holding capacity and is illustrated in Figure 3.4.

$$V_t = V_{t-1} + P - AET \tag{3.8}$$

AET is a ratio of PET, where the ratio is given by the level of the soil reservoir. The computation of AET was adapted from Kirn et al. (2017).

$$ET_a = ET_p * \frac{V_t}{V_{max}} \tag{3.9}$$

When the soil reservoir volume V_t at the time t reaches a certain threshold (V_{max}), the maximum water holding capacity of the soil, excess water defined as recharge (R) infiltrates into two parallel reservoirs.

$$R = \begin{cases} V_t - V_{max}, & \text{if } V_t > V_{max} \\ 0, & \text{otherwise} \end{cases} \tag{3.10}$$

3.4.3 Two-Parallel-Storage Model

In this study a simple linear two bucket model was used to simulate the hydraulic response of the spring in a virtual karst system to recharge events. An overview of the model is illustrated in Figure 3.4. This model can be summarised as an array of buckets or reservoirs connected in series and parallel with threshold behavior and linear outflow functions. To keep the model simple, the model has only 3 parameters (k_c, k_m and a).

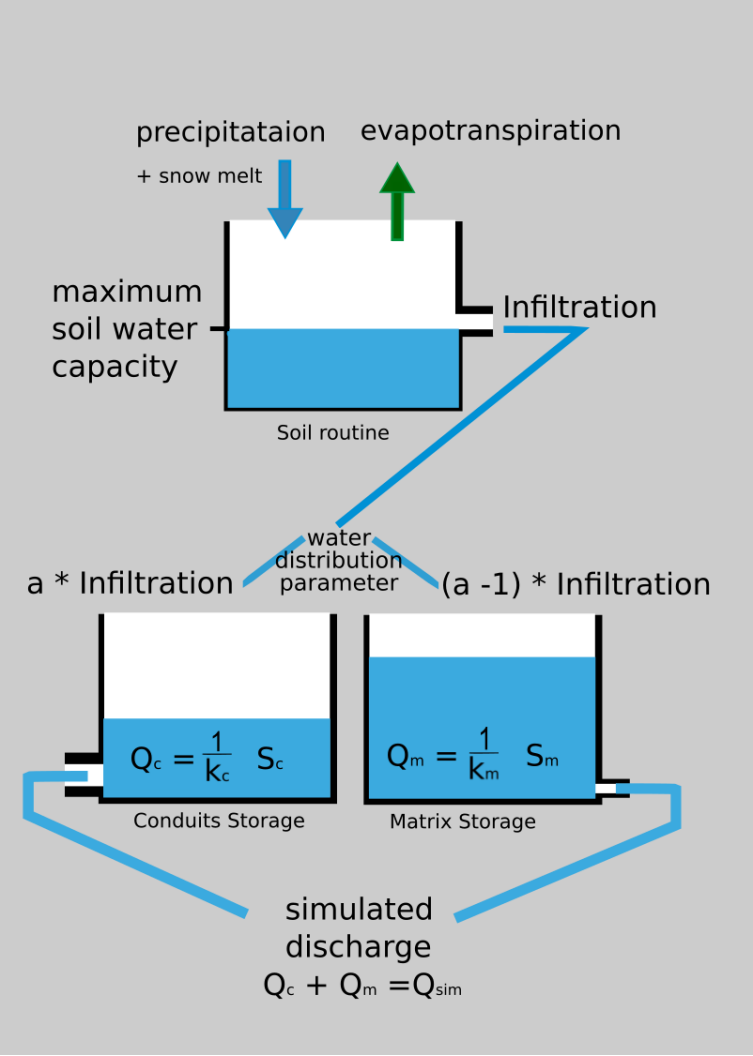

Figure 3.4: Conceptual model: Two parallel storage model and important model parameters

After the the soil is saturated, excess water (recharge) infiltrates to the groundwater. The model is a classic two parallel reservoir model with a slow and a fast draining compartment and linear outflow functions. One portion (a)

of recharge R is directed in the conduits reservoir (V_c) and the other portion $(1-a)$ flows into the matrix reservoir (V_m). Those two parallel reservoirs represent water storage in the karst conduits and in the limestone aquifer matrix, respectively.

$$V_{c_t} = R * a + V_{c_{t-1}} \tag{3.11}$$

$$V_{m_t} = R * (1-a) + V_{m_{t-1}} \tag{3.12}$$

Both reservoirs have a linear storage-outflow-function with a depletion factor of $1/k_c$ and $1/k_m$ (k_x [days] can be directly compared with the RC , see subsection 3.7.2). Both reservoirs add up to simulate final discharge.

$$Q_t = \frac{1}{k_m} * V_{M_t} + \frac{1}{k_c} * V_{C_t} \tag{3.13}$$

3.5 Model testing - "Fontaine de Vaucluse"

To test the model design and to see if the model produces reasonable results, the model was applied to input data from the catchment Fontaine de Vaucluse. The spring known as "Fontaine de Vaucluse" is located in the Provence-Alpes-Cote d'Azur region of the south of France. It is the only outlet of a carbonated formation with a drainage area of approximately 1115 km^2 and has a mean discharge of over 20 m^3/s, which makes it the largest karst spring in France. The elevation of the recharge area ranges from 200 m to over 1800 m with a mean elevation of 870 m (Fleury et al. 2007).

Discharge data from "Fontaine de Vaucluse - Moulin" were obtained from the World Karst Spring hydrograph (WoKaS) database (Olarinoye et al. 2020). Daily values of discharge [mm/d] were calculated for the period of 2004 until 2013. The data contains 58% of missing values. Precipitation and temperature datasets of the catchment were provided by Naomi Mazzilli, Assistant Professor at the Département d'Hydrogéologie at Université d´Avignon et des Pays du Vaucluse in Avignon, France. The data includes measurements from four different weather stations in the catchment at a daily resolution. Considering the elevation of the weather stations and the distribution of area in elevation classes (Table 3.3). Precipitation over the area was calculated with a weighted

average (Fleury et al. 2007).

- Mormoiron (308 m): elevation between 0 and 400 m,≈ $3,9\%$ of the recharge area.
- Sault (670 m): elevation between 400 and 800 m,≈ 37% of the recharge area.
- Saint–Christol (827 m): elevation between 800 and 1400 m,≈ 55.8% of the recharge
- Chalet Reynard (1400 m): elevation higher than 1400 m,≈ 3.3% of the recharge are

In the area precipitation was considered to fall as rainfall only, because the HBV snow routine was not available yet. Potential evapotranspiration was calculated with the same modified Thornwaite's approach (see section 3.2) and is based on the temperature measurements from the weather station Saint–Christol. Saint–Christol is located at a elevation of 827 m, which sits close to the overall average elevation of the catchment (870 m). Therefor no weighted average was used for calculating PET.

Table 3.3: Distribution of elevation classes from "Fontaine de Vaucluse" catchment in 200 m steps.
Elevation classes and surface area, adapted from Fleury et al. (2007)

Elevation class [$masl.$]	Surface area [%]
< 200	0.3
200 – 400	3.6
400 – 600	13.0
600 – 800	24.0
800 – 1000	30.0
1000 – 1200	17.5
1200 – 1400	8.3
1400 – 1600	2.6
1600 – 1800	0.7
> 1800	0.1

The input data was then fed to the model with different parameter combi-

nations. One thousand monte carlo model runs were executed with parameter ranges estimated by the results from Fleury et al. (2007) and some sensitivity analysis with dotty plots (not shown). The models warm-up period was 5 years.

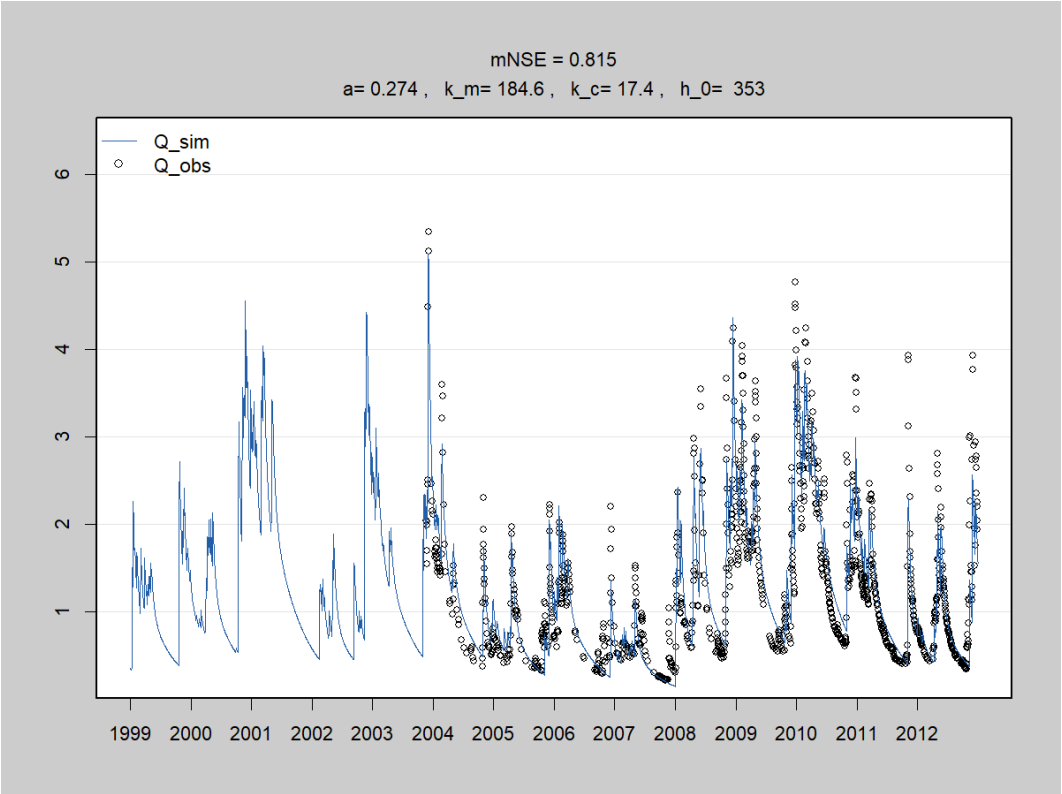

Figure 3.5: Model validation with data from Fontaine de Vauclus (Moulin), simulated discharge as blue line and observed discharge as black circles, model parameters obtained by 1000 Monte-carlo runs.

The quality of the simulation is shown by a modified Nash-Sutcliff-Efficientcy (mNSE) (Nash and Sutcliffe 1970) which is implemented in the R-package "hydroGOF". The mNSE was computed only for data pairs with no missing values. The simulated hydrograph and the observed discharge measurements are visualized in Figure 3.5. The results reached a mNSE of 0.815, which is satisfactory and sufficient enough to prove that the model can produce reasonable results when compared to discharge observations from real catchments.

3.6 Model parametrisation

All parameter of the model can be seen in the equations from the previous chapter and in Figure 3.4. Table 3.4 gives an overview of all parameter combinations

that were used in this virtual experiment to achieve the final results.

Table 3.4: Table of parameter combinations

model run nr.	k_c	k_m	a	h_0
1	100	200	0.2	50
2	50	200	0.2	50
3	20	200	0.2	50
4	5	200	0.2	50
5	100	200	0.5	50
6	50	200	0.5	50
7	20	200	0.5	50
8	5	200	0.5	50
9	100	200	0.8	50
10	50	200	0.8	50
11	20	200	0.8	50
12	5	200	0.8	50

The snow routine of the HBV model includes five more parameters (TT, CFMAX, SFCF, CFR, CWH). For every weather station used in this study a unique parameter set was extracted from the global map of HBV parameters, regionalized from Beck et al. (2016). The HBV soil routine calculates snow accumulation and melting processes for every station based on their individual parameters set.

V_{max} is the maximum soil water capacity, that was defined to be 50 mm. Higher values of V_{max} might represent real soil water capacities more accurately but for the purpose of this study we wanted to keep it as low as possible to ensure a climatic effect can be seen in the results. When increasing this parameter the buffering effect of the soil is increased significantly.

Values of 0.2, 0.5 and 0.8 were passed into a, the infiltration distribution parameter, to represent different karst systems, and can be physically interpreted as the spatial abundance of karst conduits, e.g. swallow holes at the surface. A value of 0.2 means that the karst system is not particularly abundant and only 20% of the recharge is infiltrating into the conduit groundwater storage.

k_m is the outflow parameter of the matrix storage and it is set to a fixed value of 200 days. It represents the ability of the fissured limestone rock to release water.

k_c determines the outflow from the conduit storage in the karst system. It varies during in the virtual experiment and takes values of 5, 20, 50 and 100

days. Smaller values result in a better connection of the conduit system, e.g. greater degree of karstification.

The difference of two outflow parameters should not be too small so that both reservoirs are distinguishable from each other ($k_c \ll k_m$). To make both outflow parameters more descriptive, they can also be expressed as a portion or percentage of the reservoir volume (see Table 3.5).

3.7 Recession Analysis Methods

In this work I decided to use two different recession analysis methods (RAMs), due to the great variability of methods available, meaning that using only one RAM would potentially not give sufficient results

The first RAM used in this study is based on the approach which is commonly used and suggested by the WMO (2008).

There many different recession analysis methods in the field of hydrology, but most of them are adaptations of the original recession analysis method by Brutsaert and Nieber (1977). One of most popular methods was introduced by Vogel and Kroll (1992) and is used in this study because (Stoelzle et al. 2013) showed that the approach from Vogel and Knoll most accurately filters hydrograph recession segments during baseflow conditions by applying three different methods to a selection of 20 meso-scale catchments in Germany. Following advice from this work, a slightly modified Vogel & Kroll approach was used in this study.

3.7.1 Automated Recession Segment Extraction Methods

There are many different REMs that can be used for recession analysis. They are algorithms which, apply a filter to automatically identify and select recession segments. When looking to investigate in baseflow recessions these filters minimize the effect of quickflow components.

The WMO method starts by selecting recession segments from a continuous record of discharge observations or, in this case, modeled discharge data.. Firstly, the recession is assumed to begin when the discharge falls below a certain threshold, but at least two days after peak discharge. The first part of the recession period is therefore disregarded to exclude the rapid drainage of catch-

ment storage. The threshold is defined as the 70% quantile of the discharge data. Secondly the length of the recession period has to be a minimum of seven days, to include the recession segment in the analysis. Finally, the recession segments are truncated to a certain length to be of equal length (WMO 2008).

The method based on the approach from Vogel and Knoll (1992), selects recession limbs by calculating a 3-day moving average over the decreasing part of the hydrograph. For this method it is necessary to estimate the numerical time derivative of streamflow. To account for the influence of surface runoff and stormflow this method excludes data with a discharge decline greater than 30% and the first 30% of every recession segment (Vogel and Kroll 1992). In Figure 1.1 you can see recession segments extracted by the Vogel and Kroll method in red.

It is common that the methods select recession segments by defining the starting point when dQ/dt begins to decrease and the end point when dQ/dt starts increasing again. This leads to the problem that finite different methods to estimate gradients result in error based on step-size approximations (Griffiths and Smith 2006). Divergence in the derivative of streamflow has a tremendous effect on the estimation of the recession parameters (Thomas et al. 2015). Equation 3.14 represents the most common tool in baseflow research (Brutsaert 2008). A time step of 1 (day) leads to Equation 3.15

$$dQ/dt \approx (Q_{i-\delta t} - Q_i)/\delta t \tag{3.14}$$

$$\frac{dQ}{dt} \approx Q_{t-1} - Q_t \tag{3.15}$$

3.7.2 Recession Model Fitting

All recession segments extracted by the WMO method (WMO 2008) from the record are pooled and then discharge of each time step (Q_t) is plotted against the discharge from the previous time step (Q_{t-1}).A linear model is fitted to these points. The recession model is a straight line if the recession rate follows an exponential decay, and recession parameters can be estimated by the slope ($k = Q_t/Q_{t-1}$) of this line. The recession constant C_{wmo} can be derived from k

and the size of the time step δt by the equation:

$$C_{wmo} = \frac{-\delta t}{ln(k)} \tag{3.16}$$

(WMO 2008)

This constant has the dimension of time and is directly comparable to the model parameter k_m. Finally, both values are compared and the deviation from the expected recession constant D calculates as $D_{wmo} = k_m - C_{wmo}$.

Recession segments derived from the Vogel & Kroll extraction method, are plotted ln(-dQ/dt) against ln(Q). Brutsaert and Nieber (1977) suggested fitting a lower envelope to the lowest 5% of recession data points, because only the lowest change in Q -(dQ/dt) can be related to the depletion of groundwater storage. To achieve this we used a 5% quantile regression, as suggested by Stoelzle et al. (2013). The estimator of the recession rate k can be obtained from the y-intercept of the quantile regression line (Equation 3.17) (Vogel and Kroll 1996)

$$ln(-ln(k)) = ln(-dQ/dt) - ln(Q) \tag{3.17}$$

$$k = \exp(-\exp(y - intercept)) - 0 \tag{3.18}$$

So when $ln(Q)$ is equal zero, you get a negative logarithmic change rate of Q, the y-intercept. In the example of Figure 3.6 this would be -4.800922, which will lead to recession rate k of 0.9918115 according to Equation 3.17. With this recession rate the discharge from the groundwater reservoir Q can be described as the linear outflow from a reservoir by Equation 3.19 (Vogel and Kroll 1996), where V(t) is the storage Volume at the time step t.

$$Q(t) = V(t) * -ln(k_{vog}) \tag{3.19}$$

In the example the function which describes the recession curve is,

$$Q(t) = k^t * Q_0 = 0.9918155^t * Q_0 \tag{3.20}$$

where k is the recession rate, Q is discharge at time t and Q_0 is initial discharge.

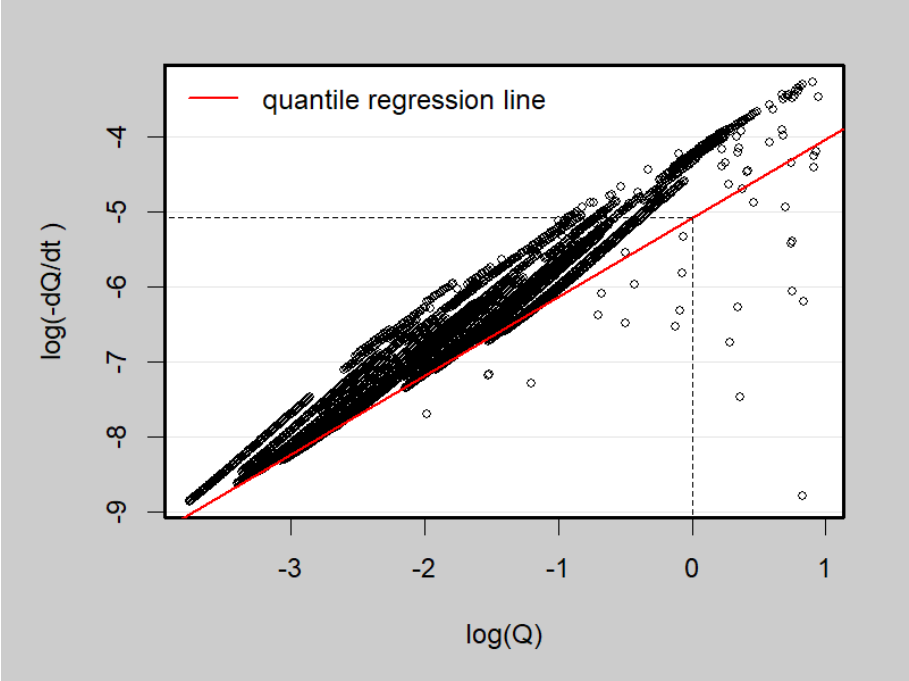

Figure 3.6: Recession points, by the Vogel & Kroll method, plotted as log(-dQ/dt) versus log(Q) and 5% quantile regression line in red, applied identification to y-intercept (dashed line)

The recession rate k_vog has to be transformed to recession constant C to be comparable with the outflow coefficient from the matrix storage k_m of the model. Therefore we equate both storage-outflow equations to Equation 3.21. The outflow function of the matrix storage is $Q_m = 1/k_m * V(t)$ (see subsection 3.4.3) and under baseflow conditions this term can be equalized to Q. And the linear recession model Equation 3.19 is based on Vogel and Kroll (1992). Solving them to k_m leads to Equation 3.22.

$$V(t) * -ln(k_{vog}) = \frac{1}{k_m} * V(t) \tag{3.21}$$

$$k_m = -\frac{1}{ln(k_{vog})} \tag{3.22}$$

Eventually, the estimated recession constant C_{vog} is $-\frac{1}{ln(k_{vog})}$ and can be compared to the model parameter k_m, which is the expected recession constant. The deviation from the expected recession constant (D) is calculate by $D_{vog} = k_m - C_{vog} = k_m + \frac{1}{log(k_{vog})}$

When considering model parameters, k_c and k_m can be linked to the linear outflow rate from the karst system and to the recession constant . Both parameters can be transformed to a recession rate by $c = e^{\frac{-1}{k}}$ and expressed as the outflow from the respective reservoir. With the unit of % per day this is more descriptive and intuitive to understand. In Table 3.5 all model parameters are transformed into recession rates and outflow rates, but for the sake of consistency I will continue to talk about recession constants C and model parameters k.

Table 3.5: Table of recession constants and recession rates

model parameter $[days]$	recession constant $[days]$	recession rate $[/day]$	outflow from reservoir $[\%/day]$
200	200	0.995	0.5
100	100	0.99	1
50	50	0.98	2
20	20	0.95	5
5	5	0.80	20

3.8 Analysis of Recession Constants

For statistical analysis of the obtained recessions constants, as well as for calculating and plotting, the application R-Studio and the Console R version 4.0.0 was used. For a more detailed look at into the analysis please see R-scripts in the supplementary materials.

Fundamentals of the statistical analysis were taken from the book "Parametrische Statistik" from Dormann (2013):

- The recession constant obtained from the virtual experiment were tested on normal distribution, with the Kolmogorov-Smirnov-Test, and Anderson-Darling-Test and the R-functions ks.test() and ad.test() respectively.
- Transformation products of the results to a link-scale with lograrhytmic an square-root transformation were tested on normal distribution the the same way.
- Kandals ranked correlations between RCs and climate indices were calcu-

lated with a function named Kendal() from the R-package "Kendal".

- To identify significant differences among the groups of RCs, the Wilcoxon-signed-rank-test was used..

4 Results

In this study a virtual experiment was conducted to asses the influence of climate and hydrology on recession based discharge analysis. To answer the hypothesis of this study, numerous recession constants were calculated by two different methods under different climate conditions and with different hydrogeological settings in a virtual experiment. First of all the two different recession analysis methods are compared to each other. Secondly the results are presented in dependence of the hydrological system for both recession analysis methods. Third the variations of recession constant against climate indices are analysed for both methods.

4.1 Influence of Hydrology on Recession Constants

The recession constants grouped by both recession analysis methods are summarized in Figure 4.1. Considering all model runs, recession constants from all parameter combinations (12) and all weather stations (814), each group contains 9768 values of recession constants. The expected value for the recession constant is the matrix recession parameter k_m introduced in the previous Chapter, and marked here as the red horizontal line at 200 days.

On comparison, the differences between the two RAMs are very clear. Whereas the Vogel & Kroll method appears to be quite precise in the majority of cases (median = 187.4), the WMO method hardly meets the expected value but systematically underestimates the recession constant. The undulating shape of the WMO violin-plot already reveals that the deviation from the k_m might be strongly related to the parametrisation of the model. The Vogel & Kroll approach is different in the sense that the results are skewed towards the lower end; Recession constants are not equally distributed around the median. The density of points is greater towards zero and gets low above the expected recession constant.

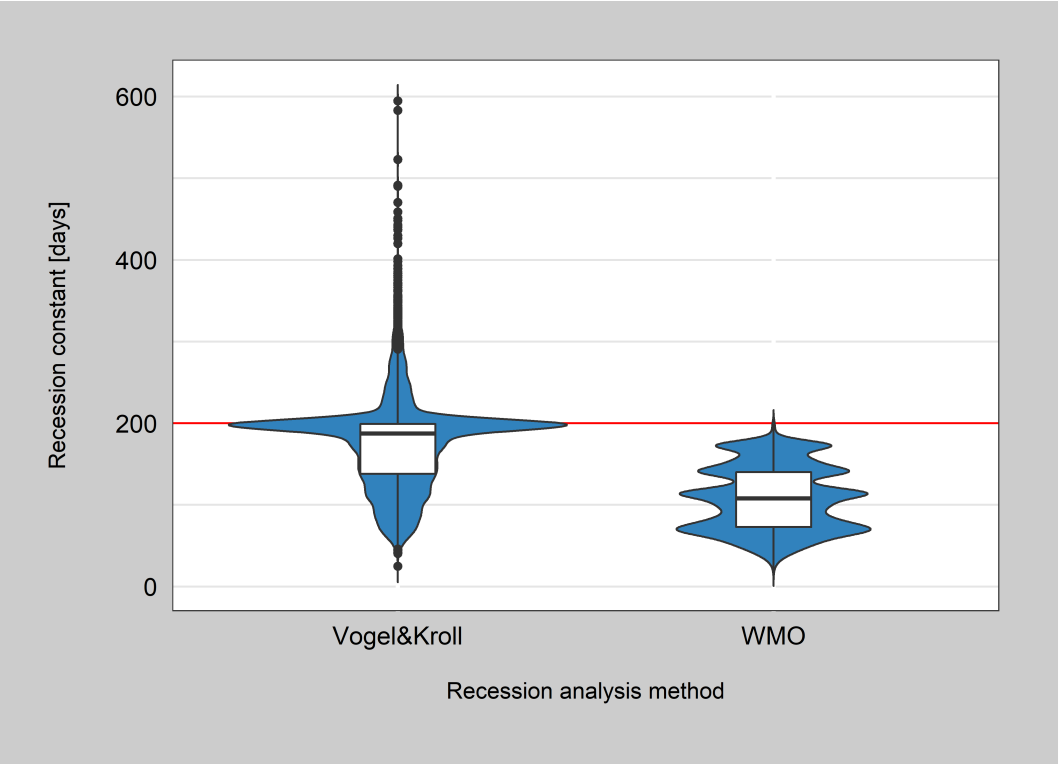

Figure 4.1: Violinplots of recession constants obtained by Vogel & Kroll method (right) and by the WMO method (left), with the expected recession constant represented by the red line

Figure 4.2 shows the variability of computed recession constants in the virtual experiment depending on the model parametrisation. The recession constants are grouped by the parameter k_c, representing the characteristics of the karst conduit network, and ranging from 100 (slow draining) to 5 (fast draining). Each boxplot includes $n = 814$ values, one for each weather station. The distribution of recession constants did not meet the preconditions for parametric statistical tests.

The boxplots of WMO recession constants, in the top compartment of Figure 4.2, show more dispersion and more deviation from the expected recession constant (red line) as the parameter k_c is set lower. On the one hand this could mean that the recession constant is more accurately defined by the WMO method when the outflow from the conduit network is low. On the other hand the IQR and whiskers of the boxplots are bigger, thus the recession constants spread out more widely. However, some outliers do fall really close to the expectancy, even closer than in scenarios with bigger k_c. Within the groups of k_c you can see the same behavior for all groups. The color scheme from light

blue to dark blue illustrates three different recharge distributions, represented by model parameter a. When the fraction of recharge to conduits gets bigger, in all groups you can see the effect of decreasing medians. The effect seems diminished for smaller k_c values. The data of all boxplots seem to be generally centered around the median. Only the outliers adumbrate that the data does not fit a normal distribution. Taking them into account, it can be said that the data is skewed towards the expected value.

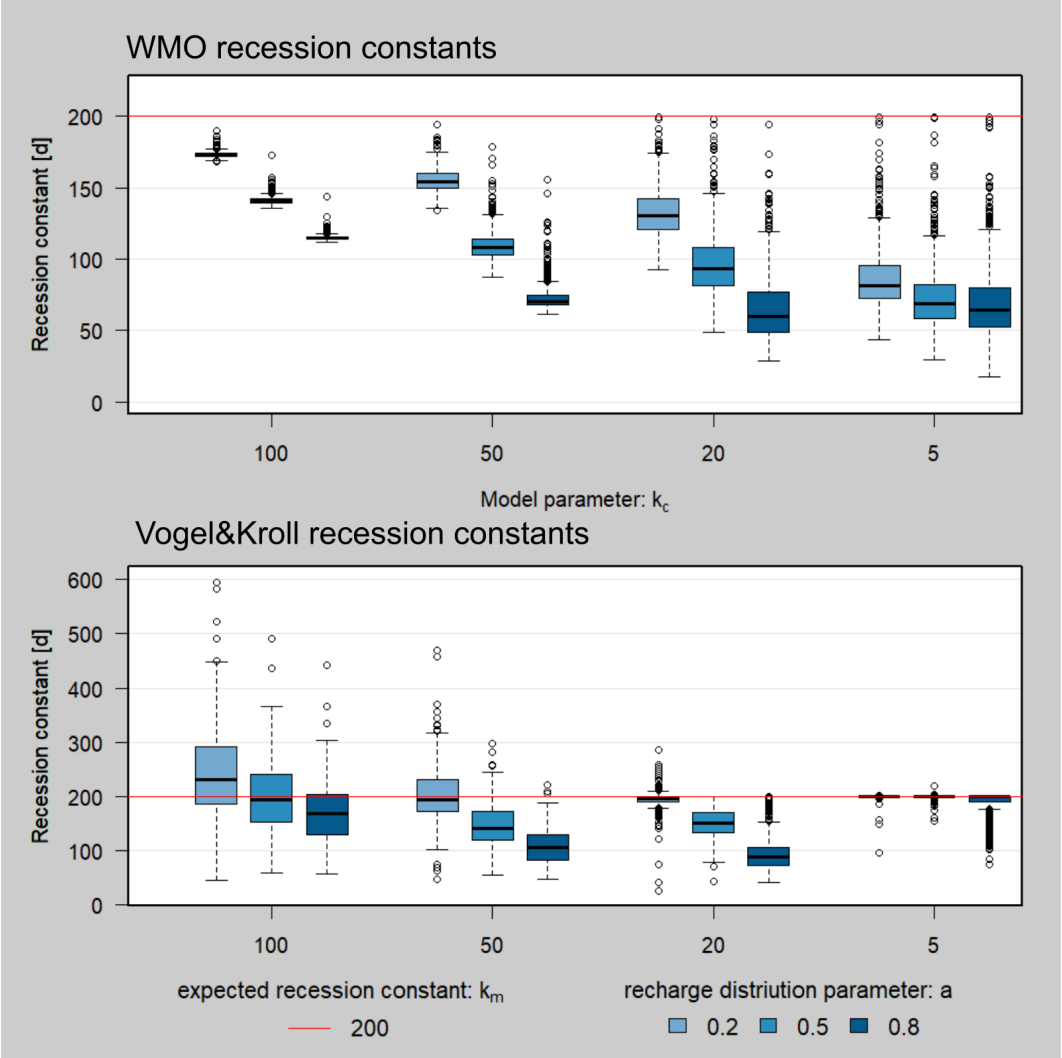

Figure 4.2: Boxplots of recession constants obtained by Vogel & Kroll method (top) and by the WMO method, divided into groups by model parameters a and k_c, with the expected recession constant represented by the red line

In the series of boxplots at the bottom, recessions constants obtained with the Vogel & Kroll method are shown. Overall they meet a greater range of recession constants (note that y-axis is scaled differently), than recession constants

from the WMO approach and they also overestimate the recession constant, which was not the case for the WMO- constants. Surprisingly they also point out a different behavior when analyzing the effect of different k_c parameters. With decreasing k_c they IQR get smaller and the medians of the recession constants get lower. The lowest deviation from the expected recession constant is found for simulations with $k_c = 5$, which represents the highest outflow from the conduits system. Median recession constants can also be close to the expected value when $a <= 0.5$. Mostly recession constants are increase when the fraction of recharge to conduits is smaller, in a similar way as the recession constant obtained by the WMO method.

In comparison, the distribution of the recession constants for the two methods look quite different in Figure 4.2. The differences are bigger between the two applied methods than the differences between in the groups of k_c and a. They share, however the behavior of smaller recession constants for when more water infiltrates into the conduit system.

4.2 Climatic Influence Recession Constants

In Figure 4.3 the deviation from the expected recession constant $D_{wmo} = k_m - c$ resulting from specific model parametrisation is plotted against the climate indices from each station included in the analysis. The four climate indices, we focused on in this study, represent the climate conditions of mostly central Europe where marine and humid climate is most abundant. For this overview of how recession constants depend on climate, a parameter combination of the model was used that could produce a reasonable degree of variations, in this case $k_c = 20$ and $a = 0.5$.

MAP plays an influence on recession parameters as shown in the first panel of Figure 4.3. The deviation from the expected recession constant increases significantly with increasing MAP, (correlation measure: Tau= 0.53) p-value = 0. The relation seems to be logarithmic, the steep increase from 250 mm per year to about 750 mm per year then flattens out beyond and approaches a limit of about 150 days asymptotically. The influence of mean annual evapotranspiration sum is less discreet. Recession constants in the second panel of Figure 4.3 circularly scatter around a median of 100 days, but there is a tendency that with increasing MAPET the deviation becomes smaller. The correlation of D_{wmo} is

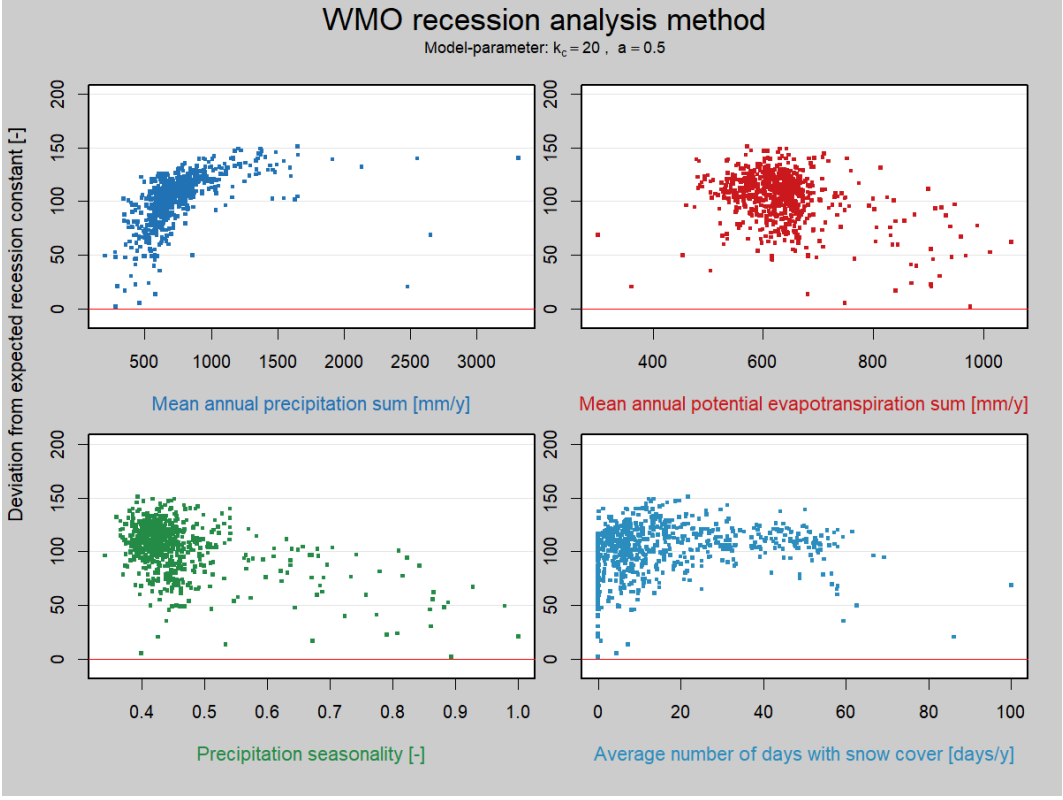

Figure 4.3: Scatterplot of deviation from expected recession constant, obtained by WMO method, against climate indices from all 814 weather stations

negative (Tau = -0.165) and also highly significant (p-value = 1.940300e-12). The function behind this dependency could be linear, however the variation is quite high within the results, thus the relation is very imprecise. A significant correlation can also be found between the WMO recession constants and precipitation seasonality (p-value = 1.540906e-19). Precipitation seasonality is bigger for longer dry periods in the year, so a negative correlation is not surprising, however with Tau = -0.224 the correlation is not very strong.

In Table 4.1 Kendall's Tau measures of correlation are displayed for each climate index and model configuration. HI was excluded here because it correlates strongly with MAPET and MAP. All calculated correlations were highly significant with p.values ranging from 0 to 0.017 and a significance level of $p = 0.05$.

The strongest correlation between climate indices and the deviation from the expected recession constant can be found for different parameter combinations. Mean annual precipitation sum correlates particularly well when the conduits recession constant is $k_c = 20$, whereas for precipitation seasonality and the

coefficient of variation in precipitation absolute value, the correlation measure is highest for model runs with $k_c = 50$ or 20. Overall the correlation measure, Tau gets bigger when the fraction of recharge to conduits (a) is bigger.

Table 4.1: Table of correlations between recession constant obtained by the WMO recession analysis from 12 different Model parametrisations and climate indices

Climate index / recession constants from specific parameter settings	precip. sum [mm]	evpo. sum [mm]	precip. seas. [-]	precip. CoV [-]	snow cover [days]
a=0.2 k=5	0.289	−0.061	−0.085	−0.171	0.056
a=0.2 k=20	0.389	−0.072	−0.109	−0.229	0.064
a=0.2 k=50	0.44	−0.145	−0.159	−0.274	0.145
a=0.2 k=100	0.386	−0.158	−0.148	−0.254	0.169
a=0.5 k=5	0.384	−0.140	−0.167	−0.264	0.124
a=0.5 k=20	**0.530**	−0.165	−0.212	−0.364	0.15
a=0.5 k=50	**0.509**	−0.181	−0.224	−0.361	0.175
a=0.5 k=100	0.456	−0.186	−0.194	−0.314	0.186
a=0.8 k=5	0.445	−0.209	−0.205	−0.31	0.19
a=0.8 k=20	**0.618**	−0.162	−0.282	−0.458	0.149
a=0.8 k=50	**0.534**	−0.195	−0.263	−0.399	0.19
a=0.8 k=100	0.453	−0.171	−0.214	−0.33	0.171

In Figure 4.4 and Figure 4.5 the deviation from the expected recession constant is plotted against precipitation related climate indices and 12 settings defining the hydrological system. The parameter settings correspond to those shown in Table 4.1. It can be seen had the relation between D_{wmo} and MAP is not linear (Figure 4.4), but seems to be logarithmic. The variation and the deviation is bigger for smaller conduit recession parameters. Also the fraction of recharge to conduits influences the deviation of WMO recession constants from the expected matrix recession constant. For $k_c = 100$ is it clearly visible that the bias in increasing with increasing a. Whereas in Figure 4.5 the influence of PSeas on D_{wmo} is negative and linear.

Plots of recession constant against other climate indices are shown in Appendix A.

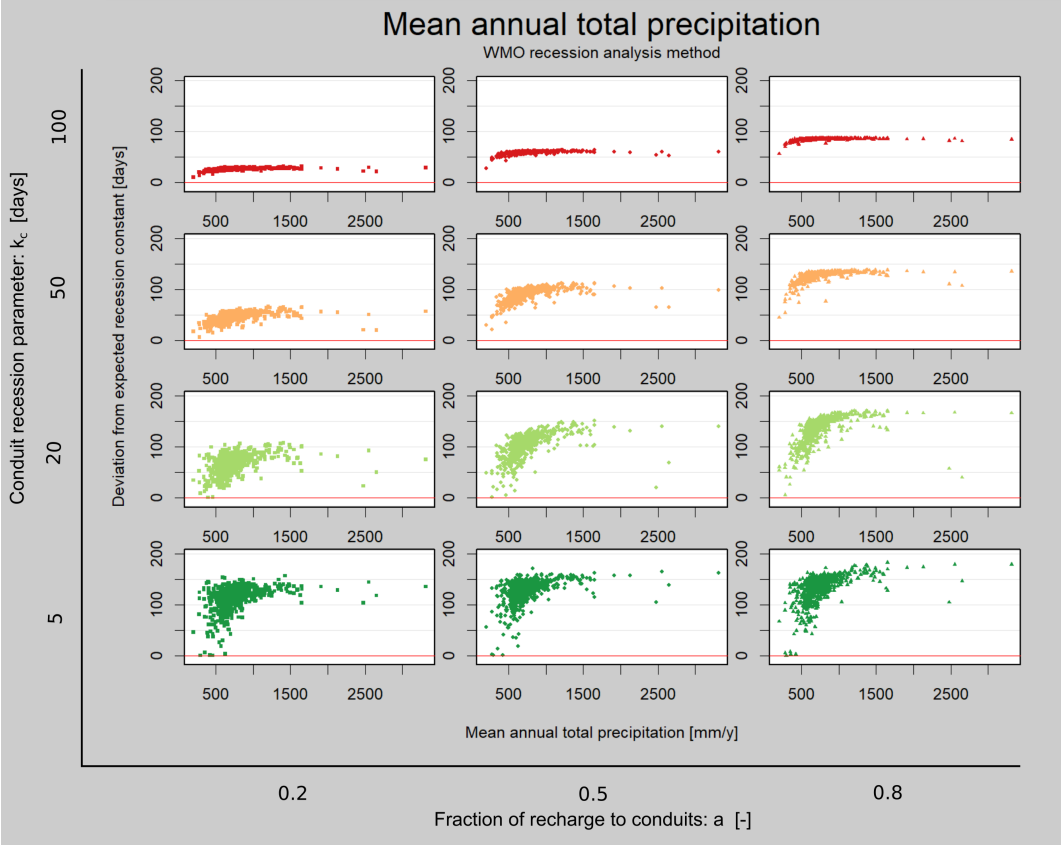

Figure 4.4: D_{wmo} plotted against MAP for diff. hydr. settings

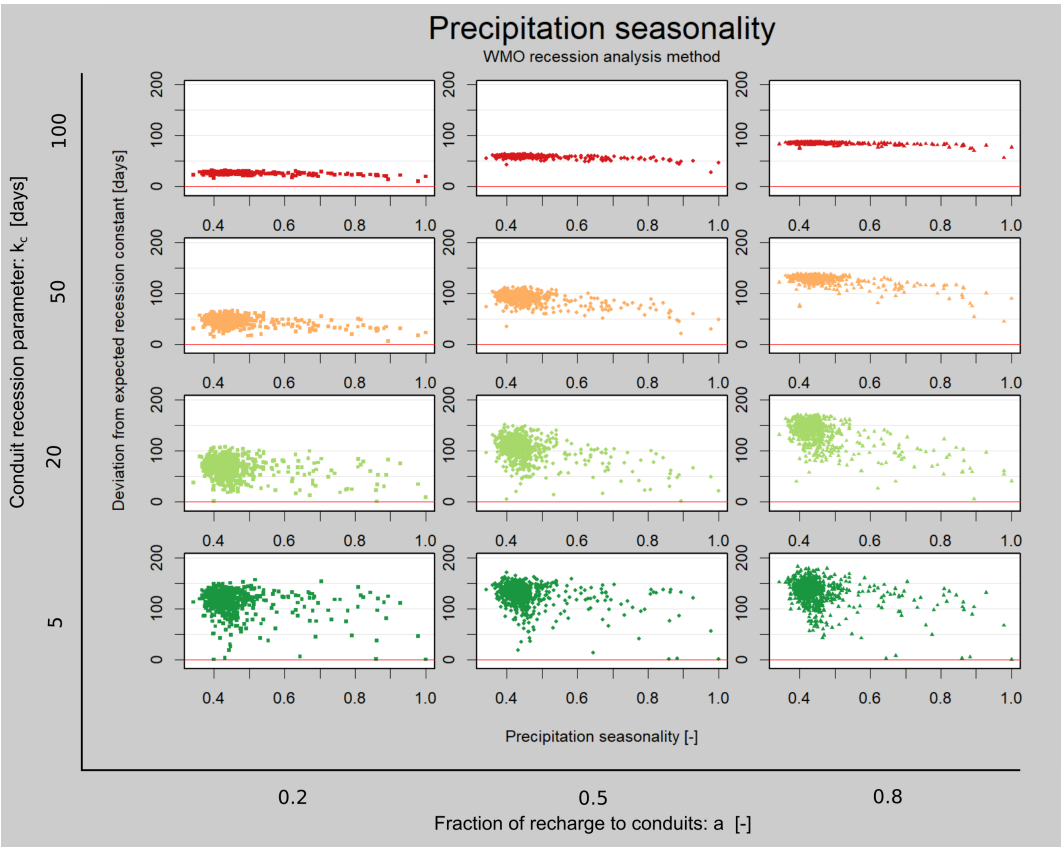

Figure 4.5: D_{wmo} plotted against PSeas for diff. hydr. settings

In Figure 4.6 the deviation from the expected recession constant $D_{vog} = k_m - C_vog = k_m = -1/k_{vog}$ as the results of model parametrisation $k_c = 100$ and $a = 0.2$ is visualized against four climate indices from each weather station.

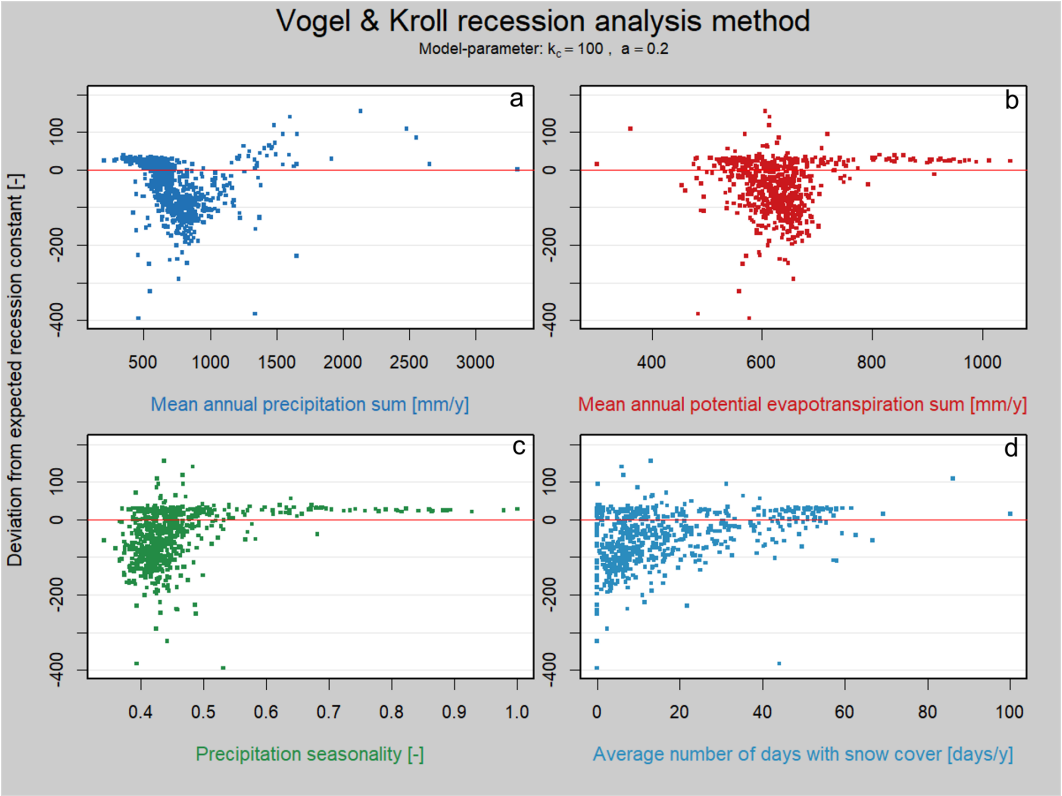

Figure 4.6: Scatterplot of deviation from the expected recession constant, obtained by Vogel & Kroll method, against climate indices from all 814 weather stations

From a visual assement of Figure 4.6 there are two overlapping patterns to be detected in the plots. In the plots b, c and d there is a continuous horizontal pattern, like a line, close to zero. In fact this "line" scatters around a deviation of 20 to 30 days. In plot a this pattern seems to start horizontally but then the deviation decreases and falls to negative. When eliminating some outliers the function of precipitation amount and the deviation hits a minimum at -200 day and then seems increases again. The other pattern is a more or less circular patterns with its center around the median of the climate index distribution. In plot c the variation of the deviation is smaller, for station with more snow cover day per year.

The relationship between precipitation seasonality in Figure 4.8 and the deviation from the expected recession constants, is not clear. The relationship

could be lograrhytmic, because the data points line up for higher Pseas close to 20 - 30 day.

Not only the scatterplots look quite different compared to the ones from the WMO method but also the correlation of the deviation from the expected recession constant with the climate indices are not homogeneous.

Correlations of climate indices with errors of the estimation of recession constant remains approximately unbiased, but may not be efficient, if the sample size is large and the population is not distributed normally. The results were tested on normal distribution but do not fit and nether their transformation products. Under these circumstances the statistical analysis is limited to none parametric test. Normality is a crucial assumption for t-test, ANOVA and generalized regression models.

In Table 4.2 Kendall's Tau measures of ranked correlations are shown for recession constants from varying parameters a and k_c with the climate indices. MAP has mostly negative correlations with recession constant as seen in Table 4.2. Positive correlation only occur for $k_c = 5$, but when considering Figure 4.7, it can be seen had the variation an deviation of recession constants is low for simulation with small k_c and a parameters. Then influence of MAP on recession constants becomes apparent when k_c is getting bigger. However the relation seem to be nether linear, nor strictly monotonous and a high degree of heroscedasticity could be seen.

Table 4.2: Table of Kendall's Tau correlations between recession constant obtained by the Vogel & Kroll recession analysis from 12 different model parametrisations and 5 climate indices

Climate index / recession constants from specific parameter settings	precip. sum [mm]	evpo. sum [mm]	precip. seas. [-]	precip. CoV [-]	snow cover [days]
a=0.2 k=5	0.327	-0.055	-0.226	-0.300	0.057
a=0.2 k=20	-0.054	-0.262	-0.046	0.056	0.346
a=0.2 k=50	-0.357	-0.171	0.218	0.368	0.285
a=0.2 k=100	-0.353	-0.111	0.283	0.407	0.229
a=0.5 k=5	**0.460**	-0.051	-0.296	**-0.406**	0.044
a=0.5 k=20	-0.042	-0.246	-0.132	0.006	0.323
a=0.5 k=50	**-0.450**	-0.166	0.213	0.418	0.285
a=0.5 k=100	-0.390	-0.106	0.288	0.435	0.231
a=0.8 k=5	**0.570**	-0.024	-0.304	**-0.468**	0.008
a=0.8 k=20	-0.242	-0.229	0.000	0.201	0.327
a=0.8 k=50	**-0.505**	-0.114	0.261	**0.485**	0.244
a=0.8 k=100	-0.407	-0.106	0.300	0.450	0.234

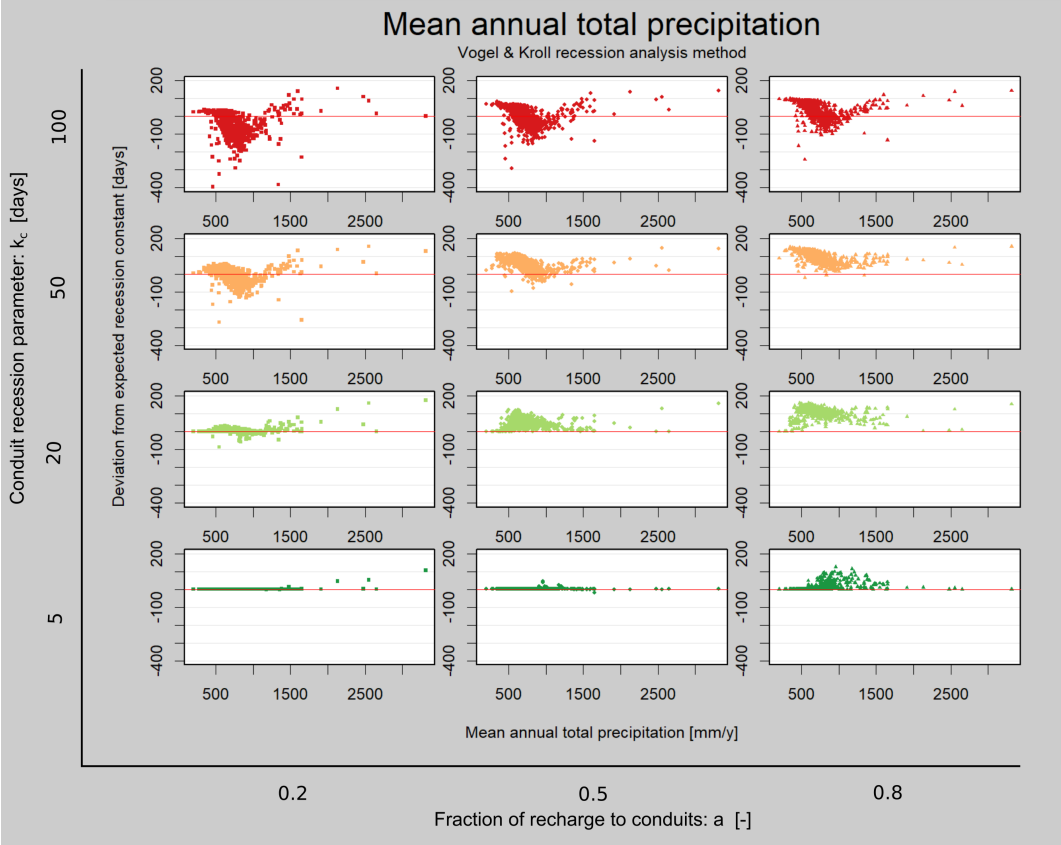

Figure 4.7: D_{vog} plotted against MAP for diff. hydr. setting

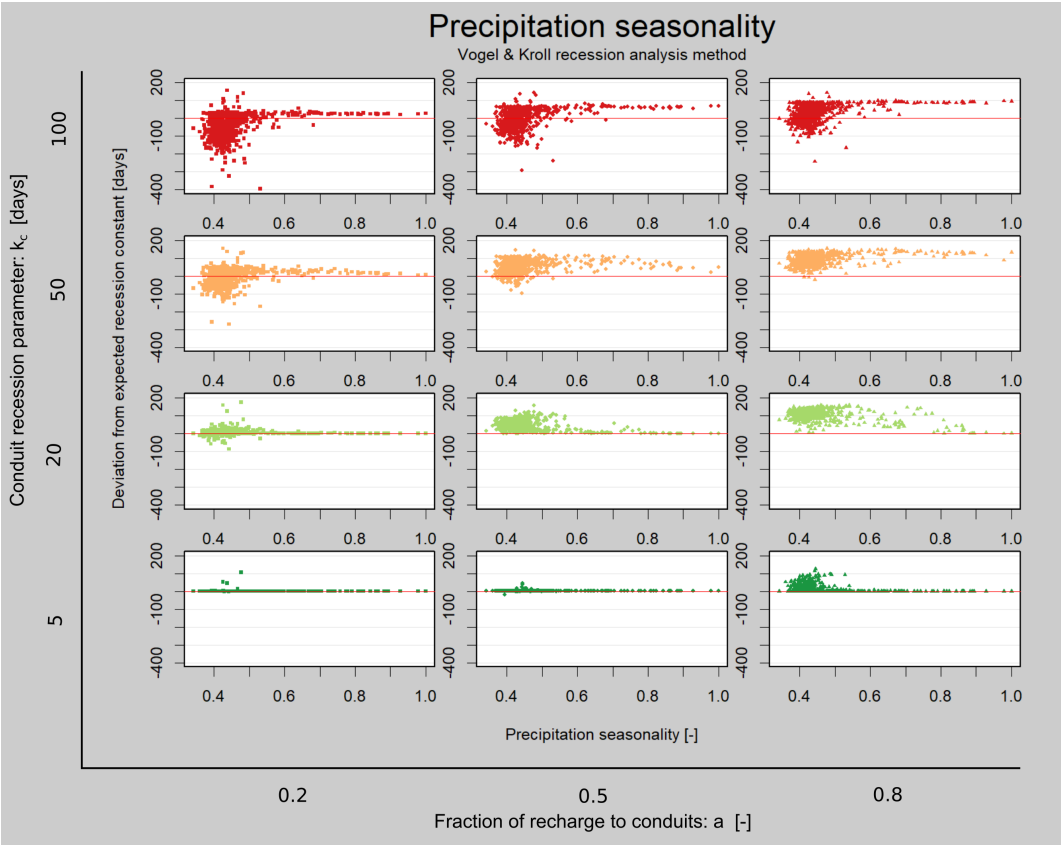

Figure 4.8: D_{vog} plotted against PSeas for diff. hydr. setting

5 Discussion

5.1 Influence of Hydrology on Recession Constants

The WMO recession constant is more accurately defined when the outflow of the karst conduit network is low, which meets the expectations that, under the influence of quickflow the baseflow recession constant deviates. With a greater outflow of the conduit storage the baseflow recession constant is superimposed by the much greater recession of the quickflow and therefor gets deviated. However, some recession constants meet the expected value better under these conditions, possible because when the conduit storage drains to almost zero (exactly zero is mathematically not possible for the model to calculate) only the matrix recession remains and this is more likely to happen if the conduit system drains fast. Therefore, under arid conditions, or when the summer recession period is long enough, a great outflow of the conduit network should lead to quite precise recession constants. This statement finds proof in Figure 4.3 and stands in line with the findings of Peña-Arancibia et al. (2010). The lowest deviations are very often located in climate which is very dry (precipitation sum < 300 mm/year) or when precipitation seasonality is high, meaning not equally distributed over the year but limited to a certain period of the year, and therefore leaving longer dry periods. The median recession constant in all boxplots of Figure 4.2 drops if the fraction of recharge to the conduit network increases. This behavior can also be explained by the superimposition of the recession of both reservoirs. The recession constant computed by the recession analysis method, gets deviated because of the influence of the conduits system. This effect is enhanced when the fraction of recharge to conduit is bigger. Matrix recession and conduit recession interfere with each other, resulting in a recession rate, between the two. This explains why the recession constant obtained by WMO method is systematically underestimated, because the computed recession constant is always a mixture of matrix and conduit recession. In Figure 4.2 the boxplots of the WMO method are always between $k_m = 200$ (matrix recession constant)

and the respective value of the conduit system (k_c =100, 50, 20, 5). Summarising the hydraulic influence on recession constant it can be said that the baseflow recession get systematically biased by the fast draining component of karst conduit system, but only if there is sufficient amount water in the conduit system.

Recession constants calculated with the recession analysis method of Vogel & Kroll have the advantage to be the most commonly studied recession characteristics and to provide recession segments which represent most accurately the groundwater or baseflow dominated part of the hydrograph. However choosing between different methods for fitting the recession model to the dQ/dt plot is an other reason why parameters of different studies can hardly be compared.

The two patterns that are identifiable in Figure 4.6 might result from two superimposed effects. The wide scatter around humid, marine climate conditions could be related to the fitting method of Vogel and Kroll (1996). The relatively unbiased line of data points over the whole range of climate conditions shifts with the fraction of recharge to the conduit system on the y-axis (Figure 4.8). The deviation gets bigger when the conduit system receives more water. Over all plots that show climate influence on the deviation of Vogel & Kroll recession constants from the expected value it can be seen that the variability of the deviation is reducing for smaller k_c. This mean that the method is more accurate when the conduits system drains faster.

Overall the correlation from the recession analysis by the Vogel & Kroll method with climate indices was not as high and explicit as the recession parameters from the WMO approach. But recession properties of the karst system are not able to be considered independent from the climate condition in which they appear.

5.2 Climatic Influence on Recession Constants

Although an climatic influence on recession parameters was found in this study, the underlying relationships could not be determined more precisely, because of non normal distributed variables. Beck et al. (2013) used a the transformation of the natural logarithm on recession parameters to fit normal distribution, but for the data of this study, this and other transformations where successful. The significant correlation between climate indices and recession constant varied

over the range applied hydrological settings and between the recession analysis methods. Overall the correlation from the recession analysis by the Vogel & Kroll method with climate indices was not as high and explicit as the recession parameters from the WMO approach. But recession properties of the karst system are not able to be considered independent from the climate condition in which they appear.

From a visual assessment of Figure 4.4 relationships between the deviation of recession constants and climate indices, in which logarithmic relationships, rather than linear relationships, could be seen.

The variability for recession parameters is in line with the findings of other studies:

- Amit et al. (2002) found exponential parameters of the recession model to be only stable in years with "normal" rainy winters and dry summers.
- Precipitation seasonality did not influence recession parameters (Beck et al. 2013; Peña-Arancibia et al. 2010)
- Relation between climate controls and recession rates where mostly charaterised by a high degree of nonlinearity and heroscedasticity (i.e. uneven variability) by Beck et al. (2013).
- Higher values of baseflow recession coefficients was found in arid catchment, whereas lower values where found in wetter catchments. When the recession constant is translated to a recession coefficient, results from Peña-Arancibia et al. (2010) can be compared with the results from this study. The role of mean annual rainfall and the humidity index in recession analysis look very similar to their plots.

5.3 Model Evaluation

Evaluating the model with discharge data from Fontaine de Vaucluse led to satisfactory results. However the model was only tested for one catchment and other catchments could perform differently in the evaluation of the model. Stoelzle et al. (2015) tested the performance of 9 different conceptual models for simulating baseflow. They found that for karst catchments the two parallel linear storage model did not perform as well as for example a linear outflow with a direct by-pass or linear outflow with threshold controlled increased

storage-outflow. Simulating baseflow to a certain degree of accuracy is crucial for accurate recession analysis. However without the two linear outflow parameters of the two-parallel-linear-storage model it is hardly possible to interpret model parameters to matrix and conduits recessions. Eventually the advantage against other model, which might perform better is the interpretation of the matrix recession constant as the expected value for the recession constant. For further investigation of this topic it might be helpful to calibrate an ensemble of different conceptual models to streamflow data and see if model parameters from other models correlate with the outflow coefficient of the matrix storage.

5.4 Limits of the Study

Some limitations of this study could be improved with futher research:

- More recession analysis methods could be considered to investigate how different REM react to the climate signal.
- More recession model parametrisation methods could be tested.
- This study focuses on linear recession model parameters, however the most fundamental recession model by Brutsaert and Nieber (1977) implies and power-law recession model with an additional non linear parameter in the exponent (see Equation 1.7).
- The errors of recession analysis could be analysed for seasonal effects. Several studies (McMillan et al. 2011; Shaw and Riha 2012) have already shown that analyzing all recession segments at once disregards the seasonal effects on recession characteristics. Also climate indices that represent seasonal pattern could be interesting to include in the analysis.
- The flied of recession based discharge analysis developed in the recent years towards the analysis of individual recession segments (Jachens et al. 2020; Shaw and Riha 2012), this could lead to very different results as this study only analysis all recession events collectively.
- The climatic influence could be characterised better if the input data would include a wider span of climate conditions. ECA-data is restricted to central Europe, with a strong focus on the Midwest and the North, and thus the range of predictors for recession analysis errors is also limited.
- Greater variety of model parameters and combinations would mean a more

continuous range of different horological systems. With more hydrological systems included it would be possible to calculate a model that predicts recession errors depending on the karstification degree.

- Prof. Jens Lange, from the Chair of Hydrology at Albert-Ludwigs-University Freiburg argued that the degree of karstification is generally linked to the amount of precipitation falling in the catchment. The process of dissolving carbonated rock with precipitation effect the hydraulic properties of the karst aquifer and therefore climate conditions could not be treated separately from the degree of karstification.
- With a fitting transformation to the data, normal distribution could possibly be achieved and thus i would be possible to apply regression models to the results. Especial predicting recession constants in dependence of model parameter a looks promising.

5.5 Outlook

We only got a first glimpse on what can be done with this model in a greater extent. One could mapped the spatial variability of recession coefficients and probably where data density is high, eg. Germany, Sweden, Norway, interpolate maps of regional climate based recession patterns. To make simulation more realistic and go towards large scale modeling, spatially distributed input data could be used for modeling recession coefficients. One could add more maps of gridded data like estimates of the maximum soil water capacity or hydraulic conductivity, shape and size of the aquifer.

Also the interest in recession analysis methods is again growing in recent past, and some new approaches have be been developed to find robust recession parameters (Delforge et al. 2020; Jachens et al. 2020; Santos et al. 2019). With those methods or a specific recession analysis method for karst spring hydrographes the virtual experiment could repeated in a slightly modified form.

6 Conclusion

This work has explored the effect of climatic properties on recession parameters of virtual karst catchments with varying degree of karstification.

Summarising the hydraulic influence on WMO recession constant it can be said that the baseflow recession gets strongly systematically biased by the fast draining component of karts conduit system. Therefore the method suggested by WMO (2008) is considered not ideal for karst spring recession analysis. The climatic influence on the deviation appears to be a logarithmic pattern which is more pronounced on recession constants obtained from the WMO approach. Evaluating the hydraulic influence on Vogel & Kroll recession parameters, the fact that this methods behaves completely different to the quickflow component stands out. Climate has a less explicit influence but the variation of recession constant is generally higher. Eventually both methods produce highly different results and thus particular attention must be paid to the choice of method for determining recession constants.

Importantly the study show the limit of of the recession analysis methods and framework for estimating their parameters. The sensitivity to estimation methods on recession parameters is once more highlighted through this study. Therefore, the flied of recession analysis in hydrology is desperately looking for simple and robust empirical framework to forecast hydrograph recession or at least a robust method for estimated recession parameter of the power-law equation from Brutsaert and Nieber (1977).

References

Amit, H., Lyakhovsky, V., Katz, A., Starinsky, A., and Burg, A. (2002). "Interpretataion of Springs Recession Curves". In: *Groundwater* 40.5, pp. 543–551.

Bagaric, I. (1978). "Determination of storage and transportation characteristics of karst aquifers". In: *Karst Hydrogeology. Water Resources Publications, Littleton, CO, USA*, p. 434.

Barnes, B. S. (1939). "The Struckture of Discharge-Recession Curves". In: *Report and Papers, Hydrology*, pp. 721–725. DOI: 10.1017/CBO9781107415324.004. arXiv: arXiv:1011.1669v3.

Basso, S., Schirmer, M., and Botter, G. (2015). "On the emergence of heavy-tailed streamflow distributions". In: *Advances in Water Resources* 82, pp. 98–105. DOI: 10.1016/j.advwatres.2015.04.013.

Beck, H., Van Dijk, A., Miralles, D., McVicar, T., Schellekens, J., and Adrian, B. (2016). "Global-scale regionalization of hydrologic model parameters". In: *Water Resources Research* 52, pp. 3599–3622. DOI: 10.1002/2015WR018247. Received.

Beck, H. E., van Dijk, A. I. J. M., Miralles, D. G., de Jeu, R. A. M., Sampurno Bruijnzeel, L. A., McVicar, T. R., and Schellekens, J. (2013). "Global patterns in base flow index and recession based on streamflow observations from 3394 catchments". In: *Water Resources Research* 49.12, pp. 7843–7863. DOI: 10.1002/2013WR013918.

Berghuijs, W. R., Hartmann, A., and Woods, R. A. (2016). "Streamflow sensitivity to water storage changes across Europe Wouter". In: *Geophysical Research Letters* 43, pp. 1980–1987. DOI: 10.1002/2016GL067927.Received.

Blume, H.-P., Brümmer, G. W., Horn, R., Kandeler, E., Kögel-Knabner, I., Kretzschmar, R., Stahr, K., and Berndt-Michael, W. (2010). *Scheffer/-Schachtschabel Lehrbuch der Bodenkunde*. Heidelberg: Spektrum Akademischer Verlag, p. 569. DOI: 10.1017/CBO9781107415324.004. arXiv: arXiv:1011.1669v3.

Bogaart, P. W., Van Der Velde, Y., Lyon, S. W., and Dekker, S. C. (2016). "Streamflow recession patterns can help unravel the role of climate and humans in landscape co-evolution". In: *Hydrology and Earth System Sciences* 20.4, pp. 1413–1432. DOI: 10.5194/hess-20-1413-2016.

Bonacci, O. (1993). “Karst springs hydrographs as indicators of karst aquifers”. In: *Hydrological Sciences Journal* 38.1, pp. 51–62. DOI: 10.1080/02626669309492639.

Borgomano, J., Masse, J. P., Fenerci-Masse, M., and Fournier, F. (2013). “Petrophysics of lower cretaceous platform carbonate outcrops in provence (SE France): Implications for carbonate reservoir characterisation”. In: *Journal of Petroleum Geology* 36.1, pp. 5–41. DOI: 10.1111/jpg.12540.

Boussinesq, J. (1877). “Theorie de l’ecoulement tourbillant”. In: *Mem. Acad. Sci.* 23, p. 46.

Brodie, R. S. and Hostetler, S. (2005). “A review of techniques for analysing baseflow from stream hydrographs”. In: *Where Waters Meet Conference*.

Brutsaert, W. (2008). “Long-term groundwater storage trends estimated from streamflow records: Climatic perspective”. In: *Water Resources Research* 44.2, p. 721. DOI: 10.1029/2007WR006518.

Brutsaert, W. and Nieber, J. L. (1977). “Regionalized drought flow hydrographs from a mature glaciated plateau”. In: *Water Resources Research* 13.3, pp. 637–643. DOI: 10.1029/WR013i003p00637.

Chen, Z., Auler, A. S., Bakalowicz, M., Drew, D., Griger, F., Hartmann, J., Jiang, G., Moosdorf, N., Richts, A., Stevanovic, Z., Veni, G., and Goldscheider, N. (2017). “The World Karst Aquifer Mapping project: concept, mapping procedure and map of Europe”. In: *Hydrogeology Journal* 25.3, pp. 771–785. DOI: 10.1007/s10040-016-1519-3.

Christensen, J. H. and Christensen, O. B. (2007). “A summary of the PRUDENCE model projections of changes in European climate by the end of this century”. In: *Climatic Change* 81.SUPPL. 1, pp. 7–30. DOI: 10.1007/s10584-006-9210-7.

Delforge, D., Muñoz–Carpena, R., van Camp, M., and Vanclooster, M. (2020). “A Parsimonious Empirical Approach to Streamflow Recession Analysis and Forecasting”. In: *Water Resources Research* 56.2, p. 5. DOI: 10.1029/2019WR025771.

Dewandel, B., Lachassagne, P., Bakalowicz, M., Weng, P., and Al-Malki, A. (2003). “Evaluation of aquifer thickness by analysing recession hydrographs. Application to the Oman ophiolite hard-rock aquifer”. In: *Journal of Hydrology* 274.1-4, pp. 248–269. DOI: 10.1016/S0022-1694(02)00418-3.

Dormann, C. F. (2013). *Parametrische Statistik, Verteilungen, maximum likelihood und GLM in R*. Ed. by H. Prof. Dr. Dette and W. Prof. Dr. Härdle. Heidelberg: Springer Spektrum, p. 350. DOI: I 10.1007/978-3-642-34786-3.

Eisenlohr, L., Király, L., Bouzelboudjen, M., and Rossier, Y. (June 1997). "Numerical simulation as a tool for checking the interpretation of karst spring hydrographs". In: *Journal of Hydrology* 193.1-4, pp. 306–315. DOI: 10.1016/S0022-1694(96)03140-X.

Fatchurohman, H., Adji, T. N., Haryono, E., and Wijayanti, P. (2018). "Baseflow index assessment and master recession curve analysis for karst water management in Kakap Spring, Gunung Sewu". In: *IOP Conference Series: Earth and Environmental Science* 148.1. DOI: 10.1088/1755-1315/148/1/012029.

Federer, C. A. (1973). "Transpiration Greatly Speeds Streamflow Recession • USDA Forest Northeastern Forest Experiment Station". In: *Water Resources Research* 9.6, pp. 1599–1604.

Fiorillo, F. (2014). "The Recession of Spring Hydrographs, Focused on Karst Aquifers". In: *Water Resources Management* 28.7, pp. 1781–1805. DOI: 10.1007/s11269-014-0597-z.

Fleury, P., Plagnes, V., and Bakalowicz, M. (2007). "Modelling of the functioning of karst aquifers with a reservoir model: Application to Fontaine de Vaucluse (South of France)". In: *Journal of Hydrology* 345.1-2, pp. 38–49. DOI: 10.1016/j.jhydrol.2007.07.014.

Ford, D. and Williams, P. (2013). "Introduction to Karst". In: *Karst Hydrogeology and Geomorphology*. John Wiley & Sons, Ltd. Chap. 1, pp. 1–8. DOI: 10.1002/9781118684986.ch1.

Grasso, D. A. and Jeannin, P.-Y. (1998). "Statistical approach to the impact of climatic variations on karst spring chemical response". In: *Bulletin d'hydrogéologie* 16, pp. 59–74.

Griffiths, D. V. and Smith, I. (2006). "Numerical Methods for Engineers". In: *Numerical Methods for Engineers*. DOI: 10.1201/9781420010244.

Hall, F. R. (1968). "Base-Flow Recessions—A Review". In: *Water Resources Research* 4.5, pp. 973–983. DOI: 10.1029/WR004i005p00973.

Hartmann, A., Goldscheider, N., Wagener, T., Lange, J., and Weiler, M. (2014). "Karst water resources in a changing world". In: *Review of Geophysics* 52, pp. 218–242. DOI: 10.1002/2013RG000443.Received.

Horton, R. E. (1933). "The role of infiltration in hydrology cycle". In: *Transactions, American Geophysical Union*, pp. 445–460.

Jachens, E. R., Rupp, D. E., Roques, C., and Selker, J. S. (2020). "Recession analysis revisited: Impacts of climate on parameter estimation". In: *Hydrol-*

ogy and Earth System Sciences 24.3, pp. 1159–1170. DOI: 10.5194/hess-24-1159-2020.

Jeannin, P.-Y. and Sauter, M. (1998). "Analysis of karst hydrodynamic behaviour using global approaches: a review". In: *Bull. Hydrogéol.(Neuchâtel)* 16, pp. 31–48.

Karlsen, R. H., Bishop, K., Grabs, T., Ottosson-Löfvenius, M., Laudon, H., and Seibert, J. (2019). "The role of landscape properties, storage and evapotranspiration on variability in streamflow recessions in a boreal catchment". In: *Journal of Hydrology* 570.December 2018, pp. 315–328. DOI: 10.1016/j.jhydrol.2018.12.065.

Kirchner, J. W. (2009). "Catchments as simple dynamical systems: Catchment characterization, rainfall-runoff modeling, and doing hydrology backward". In: *Water Resources Research* 45.2, p. 2135. DOI: 10.1029/2008WR006912.

Kirn, L., Mudarra, M., Marin, A., Andero, B., and Hartmann, A. (2017). *Improved Assessment of Groundwater Recharge in a Mediterranean Karst Region: Andalusia, Spain*. Ed. by P. Renard and C. Bertrand. P. Renard, Springer International Publishing, pp. 117–125. DOI: 10.1007/978-3-319-45465-8_13.

Klein Tank, A. M. G., Wijngaard, J. B., Können, G. P., Böhm, R., Demarée, G., Gocheva, A., Mileta, M., Pashiardis, S., Hejkrlik, L., Kern-Hansen, C., Heino, R., Bessemoulin, P., Müller-Westermeier, G., Tzanakou, M., Szalai, S., Pálsdóttir, T., Fitzgerald, D., Rubin, S., Capaldo, M., Maugeri, M., Leitass, A., Bukantis, A., Aberfeld, R., van Engelen, A. F. V., Forland, E., Mietus, M., Coelho, F., Mares, C., Razuvaev, V., Nieplova, E., Cegnar, T., Antonio López, J., Dahlström, B., Moberg, A., Kirchhofer, W., Ceylan, A., Pachaliuk, O., Alexander, L. V., and Petrovic, P. (2002). "Daily dataset of 20th-century surface air temperature and precipitation series for the European Climate Assessment". In: *International Journal of Climatology* 22.12, pp. 1441–1453. DOI: 10.1002/joc.773.

Kottek, M., Grieser, J., Beck, C., Rudolf, B., and Rubel, F. (2006). "World map of the Köppen-Geiger climate classification updated". In: *Meteorologische Zeitschrift* 15.3, pp. 259–263. DOI: 10.1127/0941-2948/2006/0130.

Kovács, A., Perrochet, P., Király, L., and Jeannin, P. Y. (2005). "A quantitative method for the characterisation of karst aquifers based on spring hydrograph analysis". In: *Journal of Hydrology* 303.1-4, pp. 152–164. DOI: 10.1016/j.jhydrol.2004.08.023.

Krakauer, N. Y. and Temimi, M. (2011). "Stream recession curves and storage variability in small watersheds". In: *Hydrology and Earth System Sciences* 15.7, pp. 2377–2389. DOI: 10.5194/hess-15-2377-2011.

Maillet, E. T. (1905). *Essais d'hydraulique souterraine & fluviale*. A. Hermann.

Malík, P. and Vojtková, S. (2012). "Use of recession-curve analysis for estimation of karstification degree and its application in assessing overflow/underflow conditions in closely spaced karstic springs". In: *Environmental Earth Sciences* 65.8, pp. 2245–2257. DOI: 10.1007/s12665-012-1596-0.

McMillan, H. K., Clark, M. P., Bowden, W. B., Duncan, M., and Woods, R. A. (2011). "Hydrological field data from a modeller's perspective: Part 1. Diagnostic tests for model structure". In: *Hydrological Processes* 25.4, pp. 511–522. DOI: 10.1002/hyp.7841.

Nash, J. E. and Sutcliffe, J. V. (1970). "River flow forecasting through conceptual models part I - A discussion of principles". In: *Journal of Hydrology* 10.3, pp. 282–290. DOI: 10.1016/0022-1694(70)90255-6.

Nathan, R. J. and McMahon, T. A. (1990). "Evaluation of automated techniques for base flow and recession analyses". In: *Water Resources Research* 26.7, pp. 1465–1473. DOI: 10.1029/WR026i007p01465.

Olarinoye, T., Gleeson, T., Marx, V., Seeger, S., Adinehvand, R., Allocca, V., Andreo, B., Apaéstegui, J., Apolit, C., Arfib, B., Auler, A., Barberá, J. A., Batiot-Guilhe, C., Bechtel, T., Binet, S., Bittner, D., Blatnik, M., Bolger, T., Brunet, P., Charlier, J. B., Chen, Z., Chiogna, G., Coxon, G., De Vita, P., Doummar, J., Epting, J., Fournier, M., Goldscheider, N., Gunn, J., Guo, F., Guyot, J. L., Howden, N., Huggenberger, P., Hunt, B., Jeannin, P. Y., Jiang, G., Jones, G., Jourde, H., Karmann, I., Koit, O., Kordilla, J., Labat, D., Ladouche, B., Liso, I. S., Liu, Z., Massei, N., Mazzilli, N., Mudarra, M., Parise, M., Pu, J., Ravbar, N., Sanchez, L. H., Santo, A., Sauter, M., Sivelle, V., Skoglund, R. Ø., Stevanovic, Z., Wood, C., Worthington, S., and Hartmann, A. (2020). "Global karst springs hydrograph dataset for research and management of the world's fastest-flowing groundwater". In: *Scientific Data* 7.1, pp. 1–9. DOI: 10.1038/s41597-019-0346-5.

Peña-Arancibia, J. L., van Dijk, A. I. J. M., Mulligan, M., and Bruijnzeel, L. A. (2010). "The role of climatic and terrain attributes in estimating baseflow recession in tropical catchments". In: *Hydrology and Earth System Sciences* 14.11, pp. 2193–2205. DOI: 10.5194/hess-14-2193-2010.

Perzyna, G. (1993). "Parameter estimation from short observation series of low flows". In: *Derived Frequency Distribution for Low Flow, DrSci. Thesis. Inst. Geophys. University of Oslo. Oslo.*

Price, K., Jackson, C. R., Parker, A. J., Reitan, T., Dowd, J., and Cyterski, M. (2011). "Effects of watershed land use and geomorphology on stream low flows during severe drought conditions in the southern Blue Ridge Moun-

tains, Georgia and North Carolina, United States". In: *Water Resources Research* 47.2. DOI: 10.1029/2010WR009340.

Rashed, K. A. (2012). "Assessing Degree of Karstification : a New Method of Classifying Karst Aquifers 1 Background". In: *Sixteenth International Water Technology Conference* 1971, pp. 1–9.

Santos, A. C., Portela, M. M., Rinaldo, A., and Schaefli, B. (2019). "Estimation of streamflow recession parameters: New insights from an analytic streamflow distribution model". In: *Hydrological Processes* 33.11, pp. 1595–1609. DOI: 10.1002/hyp.13425.

Schmidt, S., Geyer, T., Guttman, J., Marei, A., Ries, F., and Sauter, M. (2014). "Characterisation and modelling of conduit restricted karst aquifers - Example of the Auja spring, Jordan Valley". In: *Journal of Hydrology* 511, pp. 750–763. DOI: 10.1016/j.jhydrol.2014.02.019.

Seibert, J. and Vis, M. J. (2012). "Teaching hydrological modeling with a user-friendly catchment-runoff-model software package". In: *Hydrology and Earth System Sciences* 16.9, pp. 3315–3325. DOI: 10.5194/hess-16-3315-2012.

Shaw, S. B. and Riha, S. J. (2012). "Examining individual recession events instead of a data cloud: Using a modified interpretation of dQ/dt–Q streamflow recession in glaciated watersheds to better inform models of low flow". In: *Journal of Hydrology* 434-435, pp. 46–54. DOI: 10.1016/j.jhydrol.2012.02.034.

Smakhtin, V. U. (2001). "Low flow hydrology: A review". In: *Journal of Hydrology* 240.3-4, pp. 147–186. DOI: 10.1016/S0022-1694(00)00340-1.

Stoelzle, M., Stahl, K., and Weiler, M. (2013). "Are streamflow recession characteristics really characteristic?" In: *Hydrology and Earth System Sciences* 17.2, pp. 817–828. DOI: 10.5194/hess-17-817-2013.

Stoelzle, M., Weiler, M., Stahl, K., Morhard, A., and Schuetz, T. (2015). "Is there a superior conceptual groundwater model structure for baseflow simulation?" In: *Hydrological Processes* 29.6, pp. 1301–1313. DOI: 10.1002/hyp.10251.

Tallaksen, L. M. (1989). "Analysis of time variability in recessions". In: *FRIENDS in Hydrology*, pp. 85–96.

Tallaksen, L. M. (1995). "A review of baseflow recession analysis". In: *Journal of Hydrology* 165, pp. 349–370.

Thomas, B. F., Vogel, R. M., and Famiglietti, J. S. (2015). "Objective hydrograph baseflow recession analysis". In: *Journal of Hydrology* 525, pp. 102–112. DOI: 10.1016/j.jhydrol.2015.03.028.

Thornthwaite, C. W. (1948). "An Approach toward a Rational Classification of Climate". In: *Geographical review,* 38.1, pp. 55–94.

UNEP (1992). "World Atlas of Desertification, Vol. 80". In:

Van Dijk, A. I. J. M. (2010). "Climate and terrain factors explaining streamflow response and recession in Australian catchments". In: *Hydrology and Earth System Sciences* 14, pp. 159–169.

Vicente-Serrano, S. M., Beguería, S., and López-Moreno, J. I. (2010). "A Multiscalar Drought Index Sensitive to Global Warming: The Standardized Precipitation Evapotranspiration Index". In: *Journal of Climate* 23.7, pp. 1696–1718. DOI: 10.1175/2009JCLI2909.1.

Vogel, R. M. and Kroll, C. N. (1996). "Estimation of baseflow recession constants". In: *Water Resources Management* 10.4, pp. 303–320. DOI: 10.1007/BF00508898.

Vogel, R. M. and Kroll, C. N. (1992). "Regional Geohydrologic-Gemorphic Relationsships for Estimation of Low-Flow Statistics". In: *Water Resources Research* 28.9, pp. 2451–2458.

Walsh, R. P. and Lawler, D. M. (1981). "Rainfall Seasonality: Description, Spatial Patterns and Change Through Time". In: *Weather* 36.7, pp. 201–208. DOI: 10.1002/j.1477-8696.1981.tb05400.x.

Wang, D. and Cai, X. (2009). "Estimating groundwater pumping and return flow based on hydrologic recession analysis". In: *Proceedings of World Environmental and Water Resources Congress 2009 - World Environmental and Water Resources Congress 2009: Great Rivers* 342, pp. 6299–6308. DOI: 10.1061/41036(342)637.

Weisman, R. N. (1977). "The effect of evapotranspiration on streamflow recession". In: *Hydrological Sciences Bulletin* 22.3, pp. 371–377. DOI: 10.1080/02626667709491731.

White, W. B. (2002). "Karst hydrology: Recent developments and open questions". In: *Engineering Geology* 65.2-3, pp. 85–105. DOI: 10.1016/S0013-7952(01)00116-8.

Wittenberg, H. (1999). "Baseflow recession and recharge as nonlinear storage process". In: *Hydrological Processes* 13, pp. 725–726.

WMO (2008). *Manual on Low-flow Estimation and Prediction*. Vol. No, 50. 1029, p. 136.

A Appendix

Table A.1: Statistical sizes of WMO recession constant obtained from diff. hydr. settings

Statistical size / Parameter combination	Min	Q25	Median	Q75	Max	IQR
a=0.2 k=5	43.6	72.6	81.5	95.2	199.5	22.5
a=0.2 k=20	92.3	121	130.6	142.4	199.1	21.3
a=0.2 k=50	134.2	149.9	154.2	160.1	194.2	10.1
a=0.2 k=100	168.4	172.2	173.1	174.3	189.9	2.1
a=0.5 k=5	29.3	58.6	68.7	81.8	199.5	23.2
a=0.5 k=20	49.1	81.7	93.5	107.9	198	26.2
a=0.5 k=50	87.2	102.7	107.8	114.2	179	11.5
a=0.5 k=100	135.7	139.5	140.6	142.1	172.6	2.6
a=0.8 k=5	17.3	52.3	64.2	80.3	199.5	28
a=0.8 k=20	28.7	49.1	60.1	77.3	194	28.2
a=0.8 k=50	61.5	68.2	70.6	74.8	155.6	6.6
a=0.8 k=100	112	113.9	114.5	115.4	143.5	1.5

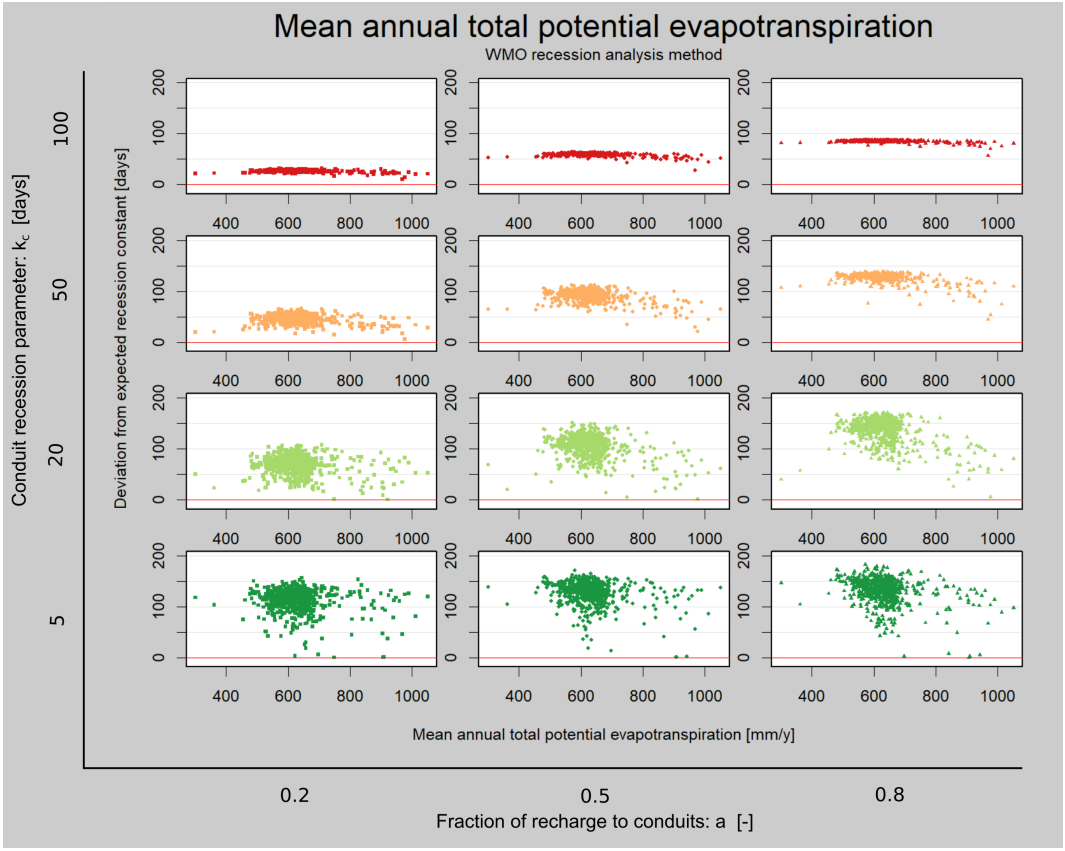

Figure A.1

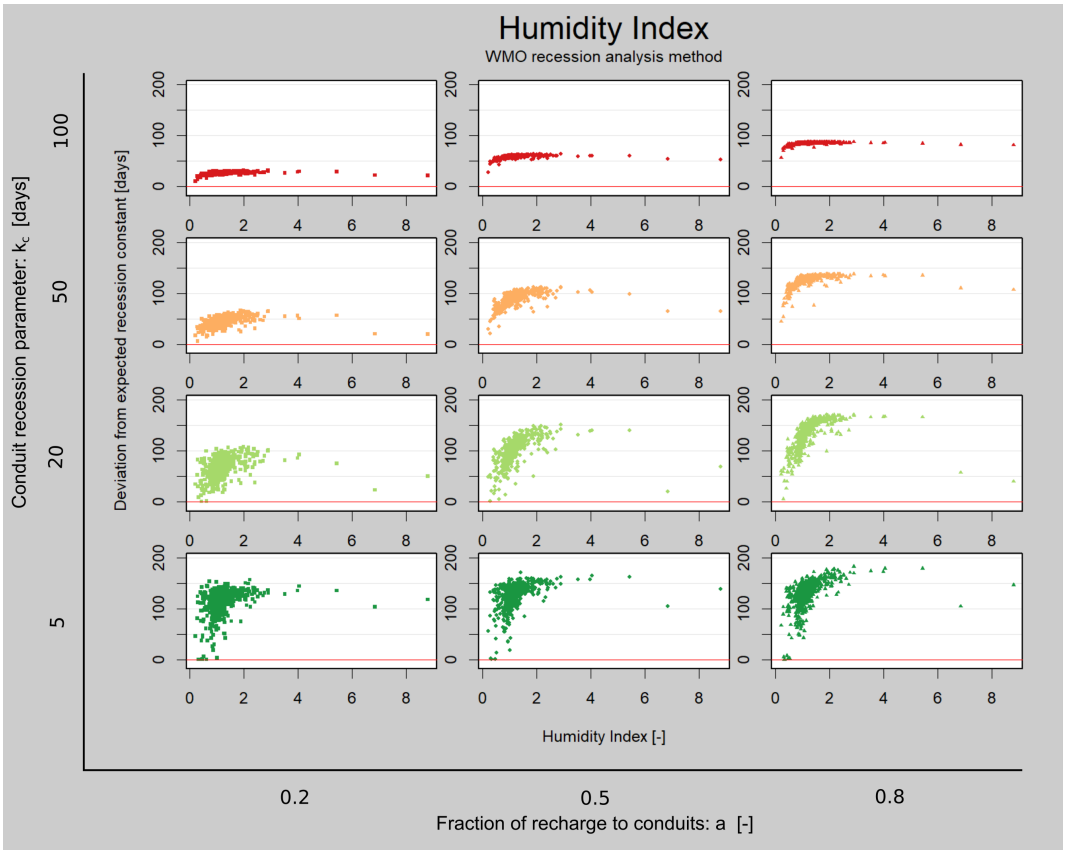

Figure A.2

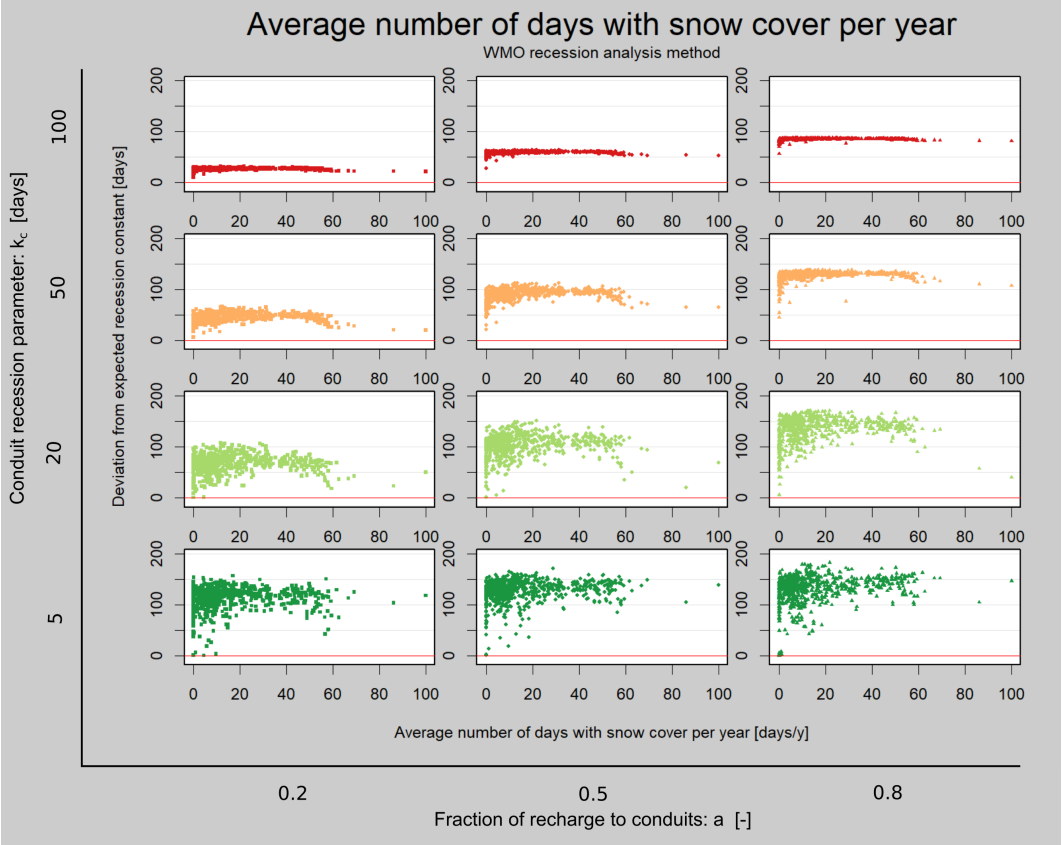

Figure A.3

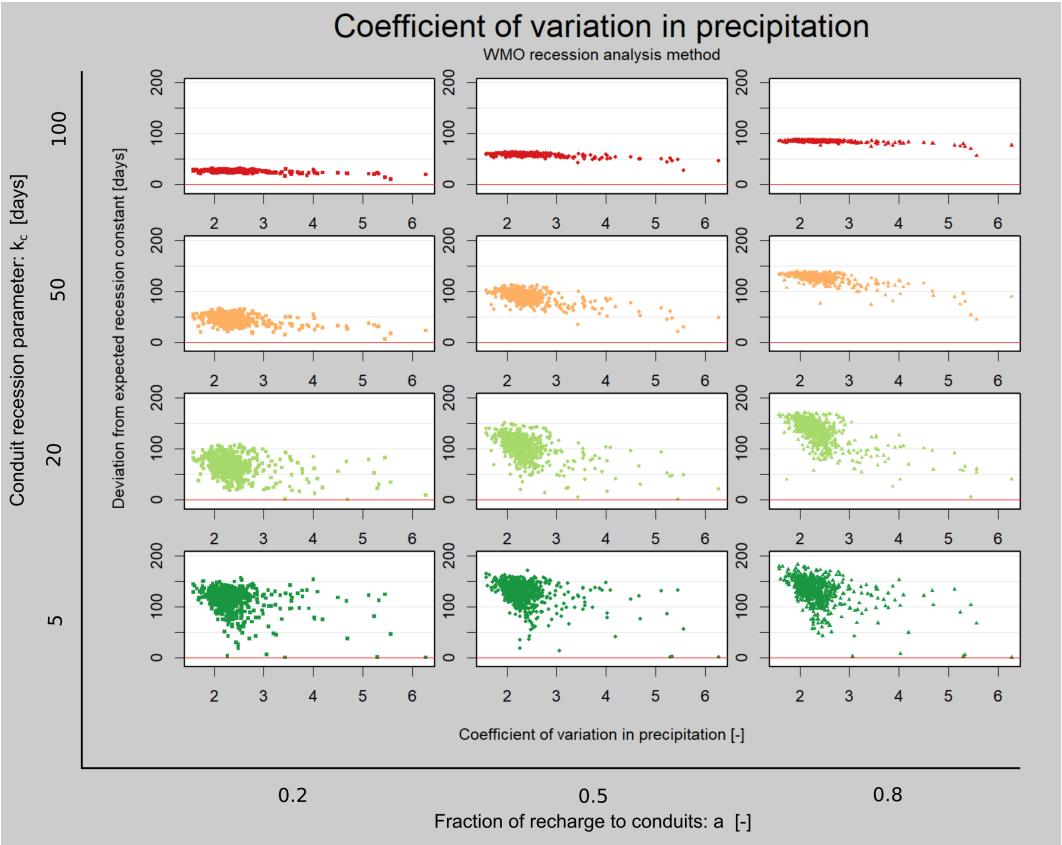

Figure A.4

B Appendix

Table B.1: Statistical sizes of Vogel & Kroll recession constant obtained from diff. hydr. settings

Statistical size / Parameter combination	Min	Q25	Median	Q75	Max	IQR
a=0.2 k=5	94.7	199	199	199	201.2	0
a=0.2 k=20	24.9	189.5	194.7	197.6	286.2	8.1
a=0.2 k=50	46	172.2	192.9	230.4	470.3	58.2
a=0.2 k=100	44.2	185.4	231.6	291.2	594.8	105.8
a=0.5 k=5	154.6	199	199	199	218.7	0
a=0.5 k=20	42.2	133.1	150.6	169.3	199.1	36.2
a=0.5 k=50	53.7	118.5	141.2	172	297.1	53.5
a=0.5 k=100	57.8	153.2	194.4	240.6	491.5	87.4
a=0.8 k=5	75.1	190	198.9	199	199.6	9
a=0.8 k=20	41.1	73.1	88.4	105.2	199	32.2
a=0.8 k=50	46.9	82.4	106.2	129.5	221	47.1
a=0.8 k=100	57.3	129.7	167.2	203.6	442.7	73.9

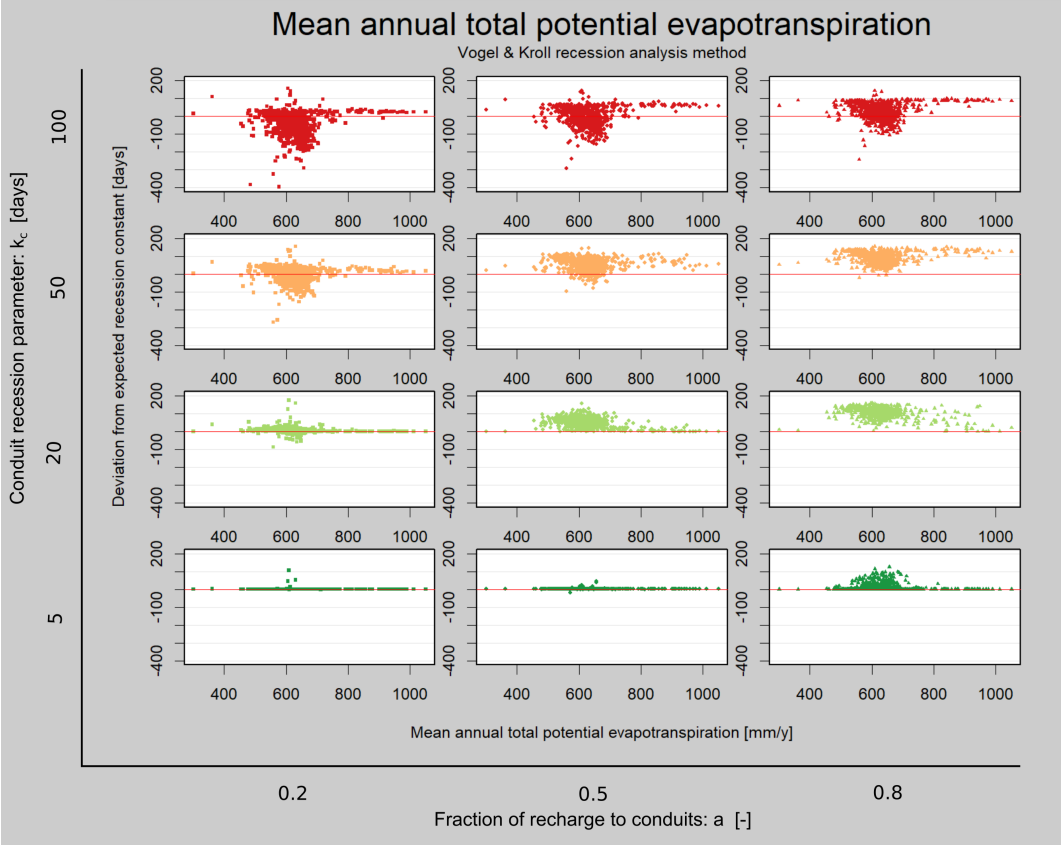

Figure B.1

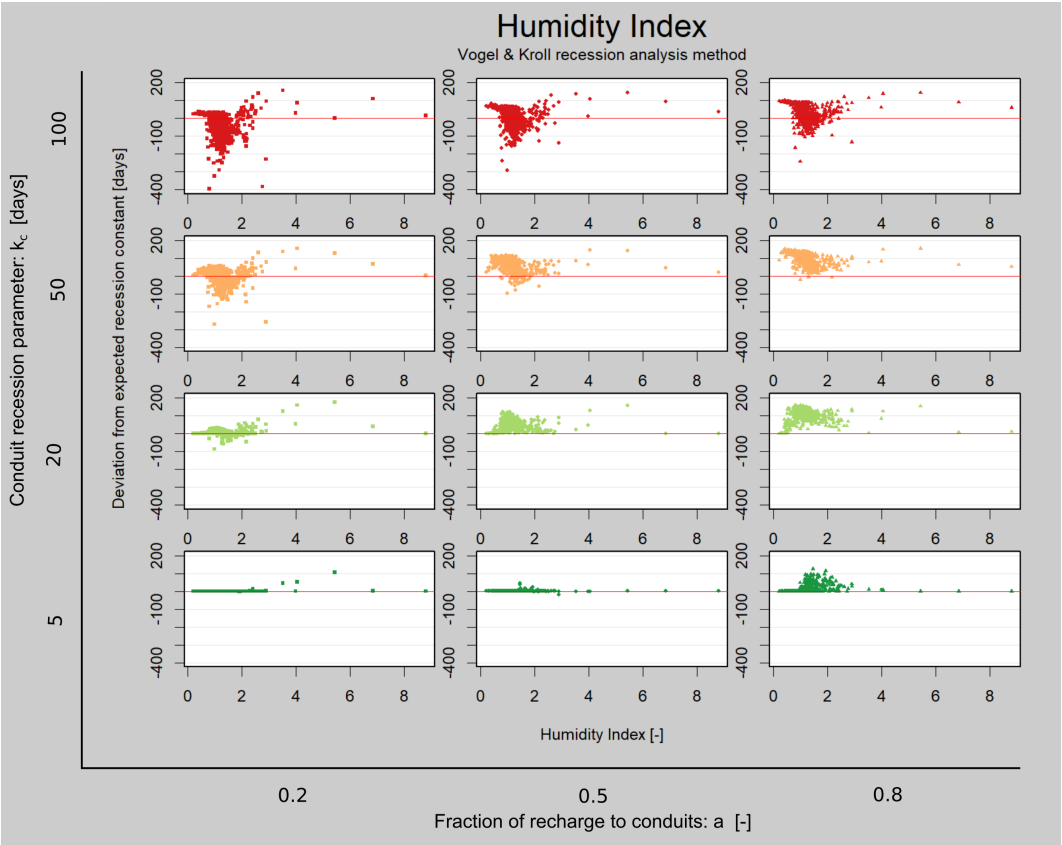

Figure B.2

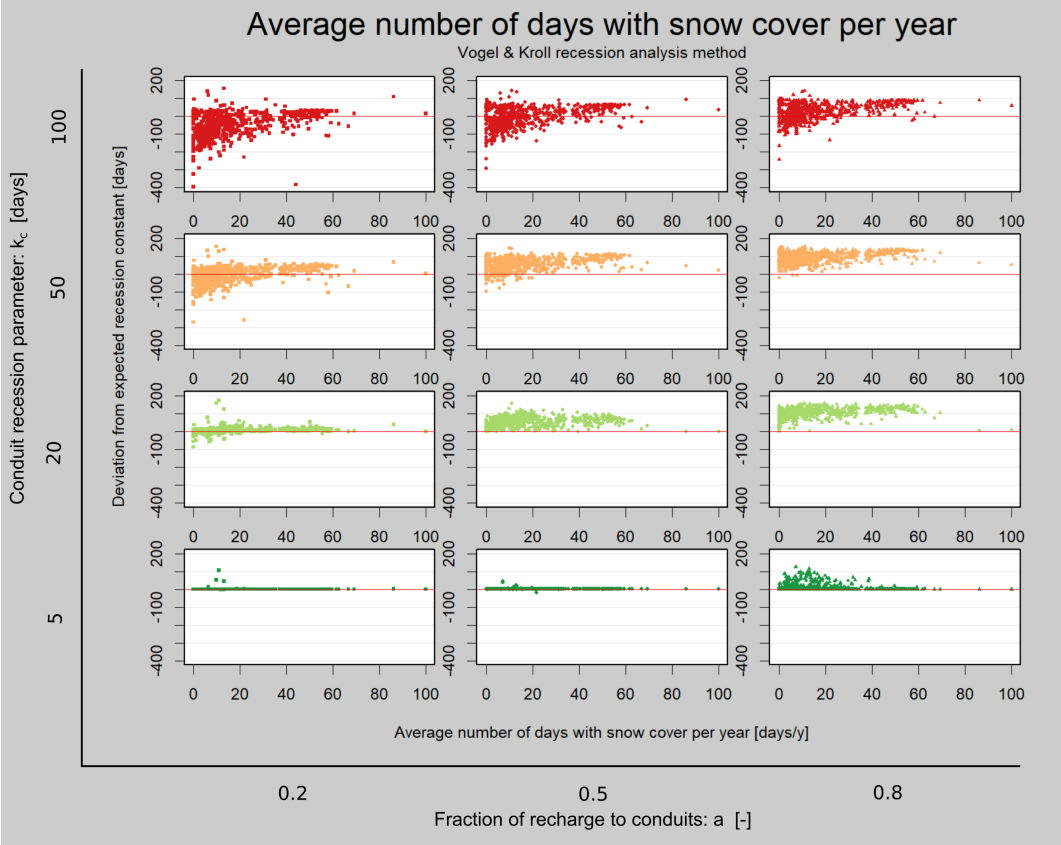

Figure B.3

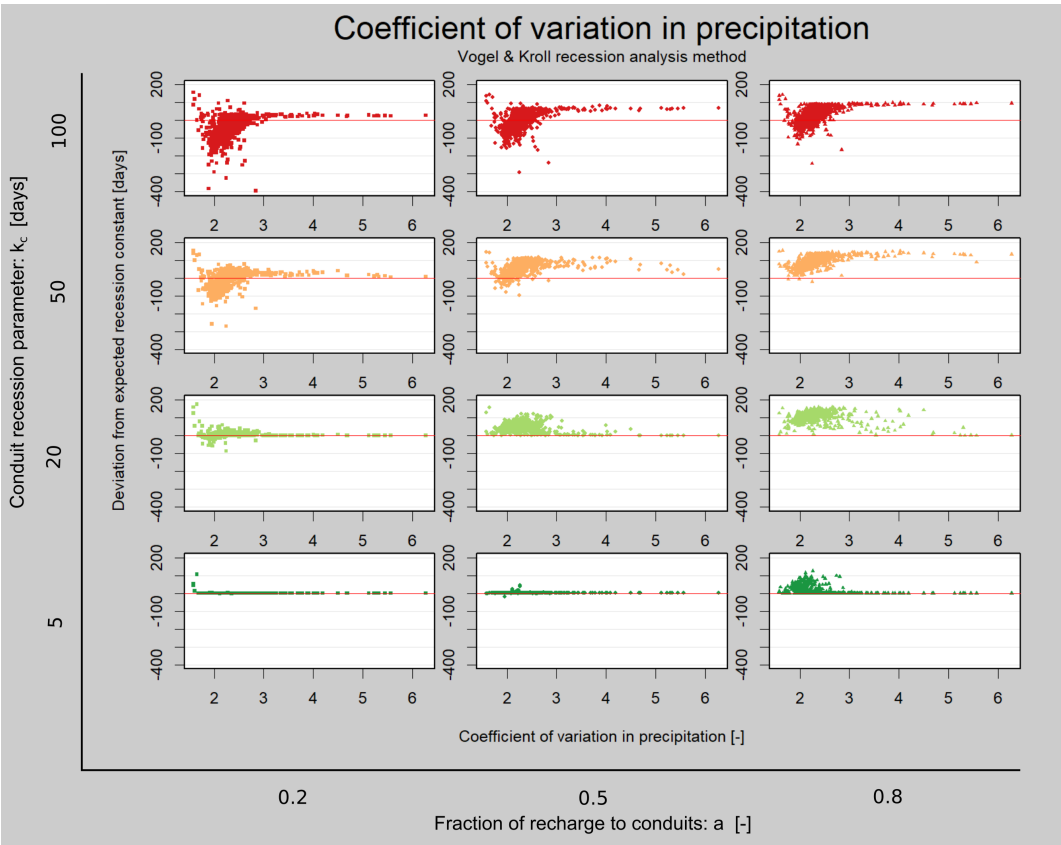

Figure B.4

Check Final Print Size

— Check final print size! —

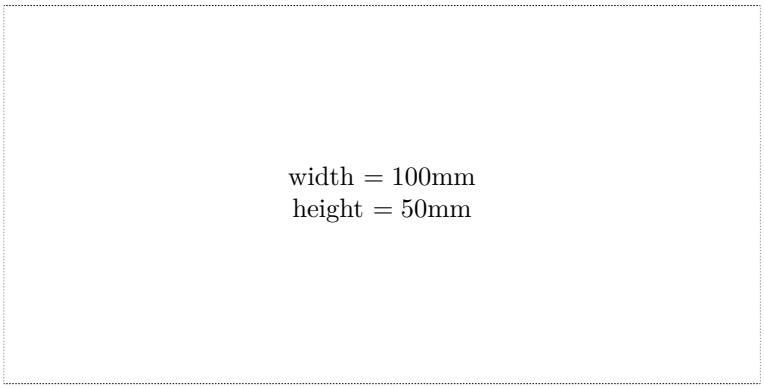

— Remove this page after printing! —